Exploiting polarised neutron and resonant x-ray reflectivity techniques to study nanoscale magnetism

@isisneutronmuon

Sean Langridge

ISIS, Rutherford Appleton Laboratory, Chilton,
Harwell Science and Innovation Campus, Oxon, United Kingdom

sean.langridge@stfc.ac.uk

Science & Technology Facilities Council ISIS

Outline

- Motivation
  - The importance of interfaces
- Reflectivity
  - Introduction to the basic Ideas
  - Information contained
    - Specular/Off-specular
  - Practical Considerations
- Examples
- Outlook
  - Bright!

Hercules Sept 2015

Science & Technology Facilities Council ISIS

Nanoscale Electronic Phenomena Research

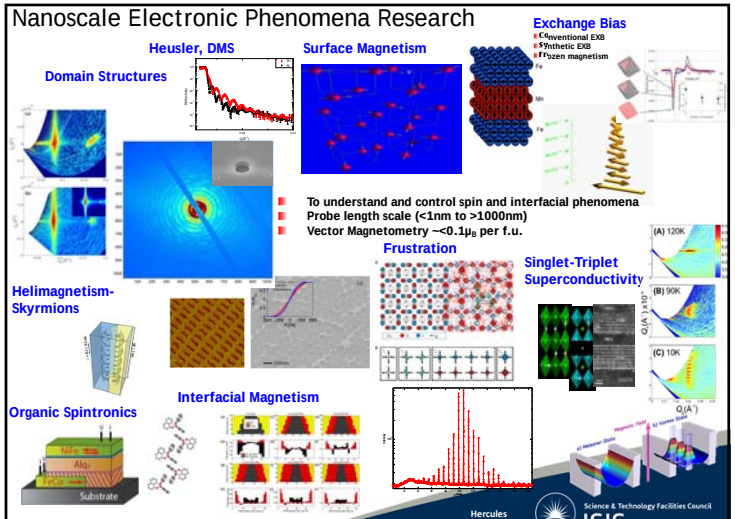

Hercules Sept 2015

Science & Technology Facilities Council ISIS

The Importance of interfaces

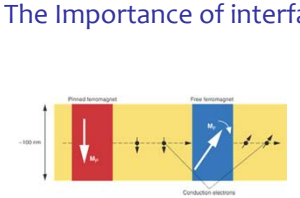

I. N. Krivorotov et al., Science **307**, 228 (2005).

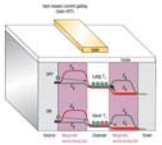

Awschalom and Flatté Nat. Phys. **3** 153 (2007)

Ramesh and Spaldin Nat. Mat. **6**, 21 (2007)

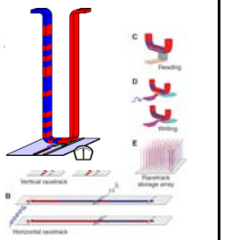

S.S.P.Parkin et al. Science **520** 5873 (2008)

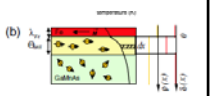

Maccherozzi et al. Phys. Rev. Lett. **101**, 267201 (2008)

Hercules Sept 2015

Science & Technology Facilities Council ISIS

Complex physics: advanced characterisation

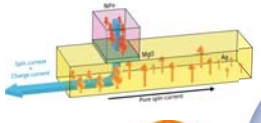

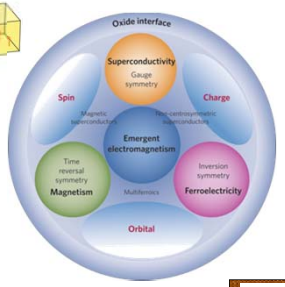

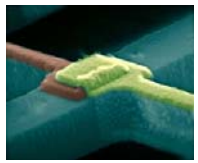

- x-section
- Polarisation
- Interfacial sensitivity

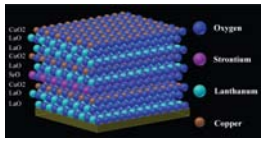

Nat. Phys. 7, 75–79 (2010)

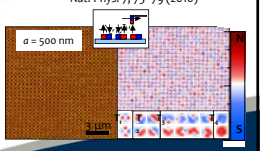

Nature Materials 11, 103–113 (2012)

Science & Technology Facilities Council ISIS

Complementarity

- Bulk measurements
  - Magnetometry
  - Transport...

- X-rays
  - Element specific
  - Shell Selective
  - Good Q-resolution
  - Weak interaction
  - High incident flux
  - Large resonant enhancements
  - Strong absorption (resonant)
  - Polarisation dependence
  - Small coherence length (<10μm)
- Imaging
  - XPEEM
  - Lorentz
- Neutrons
  - Strong magnetic scattering
  - Penetrative probe
  - Good energy resolution
  - Absolute measurement
  - Polarisation analysis
  - Long coherence length (~100μm)

Science & Technology Facilities Council ISIS

Interference effects

- Fresnel reflection 1815

Neutrons & Magnetism

Science & Technology Facilities Council ISIS

Scattering from a single (fixed) atom

- atomic nuclei via the short-range (fm) strong force;
- unpaired orbital electrons via a magnetic dipole interaction

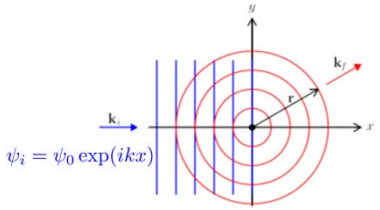

Scattering length

$$\sigma_{tot} = 4\pi b^2$$

Where *b* is the scattering length

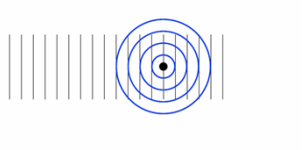

- The sign of *b* is arbitrary
- A negative sign implies a change in the phase of the scattered wave
- *b* is sometimes complex and wavelength dependent due to resonant absorption
- *b* depends on the isotope
- *b* depends on the spin states of the neutron and nucleus

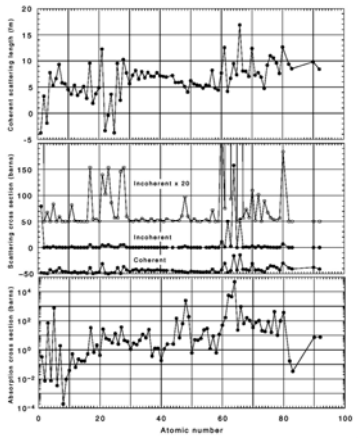

- Mass 1.67 x 10^{-27}kg 1.008665 atomic units
- Charge 0 (1.5 ±2.2) x 10^{-22}proton charge
- Spin ½
- Magnetic moment -1.913μ_N
- Electric dipole moment < 6 x 10^{-25}e-cm

$$\lambda = \frac{h}{mv}$$

$$E = \frac{h^2}{2m\lambda^2}$$

Isotope Dependence

Nickel Isotope	Scattering length *b (fm)*
^{58}Ni	15.0(5)
^{60}Ni	2.8(1)
^{61}Ni	7.60(6)
^{62}Ni	-8.7(2)
^{64}Ni	-0.38(7)

Hydrogen Isotope	**Scattering length *b(fm)***
1H	-3.7409(11)
2D	6.674(6)
3T	4.792(27)
O	5.803

$$|11\rangle = \uparrow\uparrow$$
$$|10\rangle = (\uparrow\downarrow + \downarrow\uparrow)/\sqrt{2}$$
$$|1\ -1\rangle = \downarrow\downarrow$$
$$|00\rangle = (\uparrow\downarrow - \downarrow\uparrow)/\sqrt{2}$$

- Isotopic substitution for contrast
- Isotopic substitution to move peak positions in spectroscopy
- Incoherent scattering

SLD

http://www.ncnr.nist.gov/resources/sldcalc.html

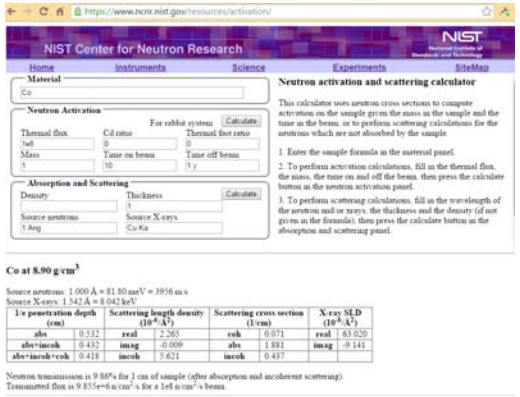

Neutrons and Magnetism

- B-field due to both orbit and spin

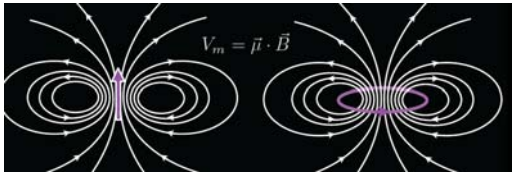

- The neutron has a magnetic moment
  - Can solve magnetic structures
  - Can study magnetic excitations

Field due to spin and orbital moments is

$$\vec{B} = \vec{B}_s + \vec{B}_L = \frac{\mu_0}{4\pi}\left\{\vec{\nabla} \times \left(\frac{\vec{\mu}_e \times \hat{R}}{R^2}\right) - \frac{2\mu_B}{\hbar}\frac{\vec{p} \times \hat{R}}{R^2}\right\}$$

Magnetic vector potential $\vec{A}$, of a dipolar field due to electron spin moment

Biot-Savart Law for a single electron of linear momentum, $\vec{p}$

Evaluating the spatial part of the transition matrix element

$$< \vec{k}_f|V|\vec{k}_i > \propto \exp(i\hat{Q}\cdot\vec{r}_k)\left\{\hat{Q} \times \left(\vec{s}_j \times \hat{Q}\right) + \frac{i}{\hbar Q}\left(\vec{p} \times \hat{Q}\right)\right\}$$

Basic Ideas

- Magnetic dipole moment:
- Differential cross-section

$$\boldsymbol{\mu}_n = -\gamma \frac{e\hbar}{2m}\boldsymbol{\sigma}$$

$$\frac{d^2\sigma}{d\Omega dE} = \frac{k'}{k}\left(\frac{m}{2\pi\hbar^2}\right)^2 \left|\left\langle k'\sigma'\lambda'\middle|V_m\middle|k\sigma\lambda\right\rangle\right|^2 \delta\left(E_\lambda - E_\lambda' + \hbar\omega\right)$$

(See *e.g.* Squires eqn 7.15)

$$\hat{V}_m = -\hat{\boldsymbol{\mu}}_n \bullet \mathbf{B}$$

$$\left\langle k'\middle|\hat{V}_m\middle|k\right\rangle = -r_0\hat{\boldsymbol{\sigma}} \bullet \hat{\mathbf{Q}}_\perp$$

$$\hat{\mathbf{Q}}_\perp = \sum_i \exp(i\boldsymbol{\kappa} \bullet \mathbf{r})\left(\boldsymbol{\kappa} \times (\hat{\mathbf{s}}_i \times \boldsymbol{\kappa}) - \frac{i}{\hbar\kappa}(\boldsymbol{\kappa}_i \times \hat{\mathbf{p}}_i)\right)$$

$$\mathbf{Q} = -\frac{1}{2\mu_B}\mathbf{M}(\boldsymbol{\kappa})$$

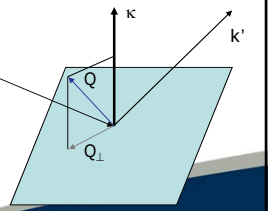

$$Q = Q_s + Q_l = \frac{1}{2\mu_B}\mathrm{M}(\kappa)$$

- Neutrons only see the components of the magnetisation perpendicular to the scattering vector

- 1972 first non-resonant magnetic x-ray scattering experiment by Bergevin and Brunel
- 1985 first prediction of magnetic resonance scattering by Blume
- 1985 first experimental observation of resonance enhancement at the K-shell of Ni by Namikawa *et al.*
- 1987 discovery of resonance absorption of circular polarized x-rays in Fe by G. Schütz *et al.*
- 1988 seminal paper by Gibbs et al. on magnetic scattering at Ho spin spiral
- 1990 first demonstration of resonance magnetic reflectivity at Fe –film by Kao *et al.*

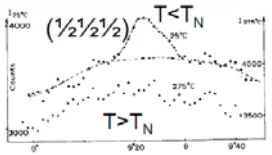

Fig. 1. Intensity $I_{(\delta)}$ near the $(\frac{1}{2}\frac{1}{2}\frac{1}{2})$ position at $t = 25°$ C and 275° C in counts/225 min. The hump which cover the interval could be due to some impurity.

Non-resonant Spin term

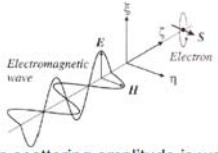

E-field interacts with the charge, but H-field interacts with the spin of the electron. This gives rise to a weak spin scattering amplitude with the following characteristics:

- Spin scattering amplitude is weaker than charge scattering by a factor: $\tau = h\nu/m_e c^2 = E_{Photon}/E_{electron} \approx 10keV/511keV = 2\times10^{-2}$
- For a single electron the intensity is reduced by $\tau^2 \approx 10^{-4}$, such that only with high energy x-rays non-resonant spin scattering makes sense.
- Charge and spin scattering for a plane polarized incident beam are 90° out of phase
- Spin scattering causes a partial rotation of the plane of polarization
- The combined charge and spin scattering amplitude becomes:

$$f = -r_e\left[(\boldsymbol{e}_f \cdot \boldsymbol{e}_i)F_c - i\tau\, \boldsymbol{F}_s \cdot \boldsymbol{B}\right]$$

Non-resonant orbital term

Scattering of EM-waves at atoms slightly changes the orbit of electrons, giving rise to orbital magnetic scattering. The combined charge and spin and orbitatl scattering amplitude becomes:

$$f = -r_e\left[(\boldsymbol{e}_f \cdot \boldsymbol{e}_i)F_c - i\tau\left[\boldsymbol{F}_s \cdot \boldsymbol{B}_s + \boldsymbol{F}_l \cdot \boldsymbol{B}_l\right]\right]$$

$\boldsymbol{F}_{c,s,l}$ are unit cell structure factors for the charge, spin, and orbital distribution, respectively.

$\boldsymbol{B}_{s,l}$ express selection rules, similar to magnetic neutron scattering, such that the cross section are only sensitive to magnetic moments, which are perpendicular to the scattering vector.

However, $\boldsymbol{B}_s$ and $\boldsymbol{B}_l$ describe different rotations of the plane of incident polarization, which allows a separation of spin and orbital contributions, unlike neutron scattering.

Non-Resonant Summary

- Magnetic scattering of spin and orbital moment rotates the plane of polarization, but differently, allowing separation of spin and orbital contributions; for forward scattering, orbital sensitivity is lost. Spin scattering is therefore best achieved by using high energy x-rays at small scattering angles.
- For a linearly polarized incident wave, the scattering amplitudes of charge and magnetic scattering (spin and orbital) are 90° out of phase. Because of the π/2-shift, charge and magnetic scattering can not interfere (interference term can not be used for scattering enhancement);
- Magnetic scattering is very weak compared to charge scattering. The magnetic cross section scales with τ^2. (In the case of the Brunel& de Bergevin experiment the intensity ratio was about 10^{-7}!) $(e^2/mc^2)^2$
- Magnetic and charge scattering can either be separated in case of an antiferromagnetic reflection (NiO), or by σ–π scattering.

Example UAs

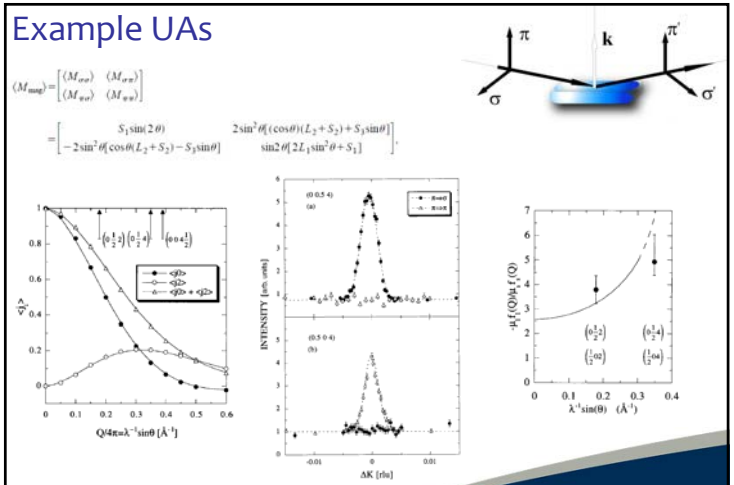

Resonance Enhancement

- Core level spectroscopy

$\Delta l = \pm 1$

$\Delta m = \pm 1$

$\Delta S = 0$

Co	L_{II}	L_{III}
	$2p_{1/2} \Rightarrow d$	$2p_{3/2}$
	793.2eV	778.1eV

$$f_n^{res} = \begin{pmatrix} 1 & 0 \\ 0 & \mathbf{k_i}\cdot\mathbf{k_f} \end{pmatrix} F_n^{(0)} + i \begin{pmatrix} 0 & -\mathbf{k_i}\cdot\mathbf{M_n} \\ \mathbf{k_f}\cdot\mathbf{M_n} & (\mathbf{k_i}\times\mathbf{k_f})\cdot\mathbf{M_n} \end{pmatrix} F_n^{(1)}$$

$$I = Tr(\vec{f_n^{res}}\cdot\rho\vec{f_n^{res}}^{*})$$

Hannon, J. P., *et al.* 1988, *Phys. Rev. Lett.* **61**, 1245
J. P. Hill and D. F. McMorrow, Acta Crystallogr., Sect. A: Found. Crystallogr. **52**, 236 (1996)

- Transmission

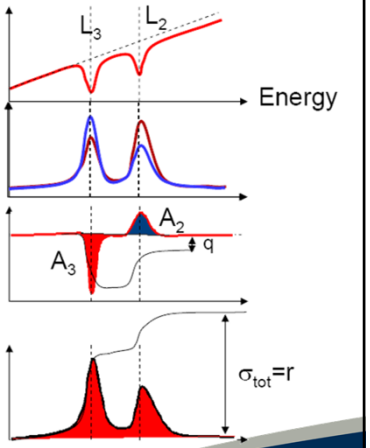

- Difference signal

$$q = \int (\mu_+ - \mu_+) dE$$

- ∝orbital moment
- Total absorption

$$r = \int (\mu_+ + \mu_+) dE$$

XMCD absorpton spectrum

XMCD difference spectrum

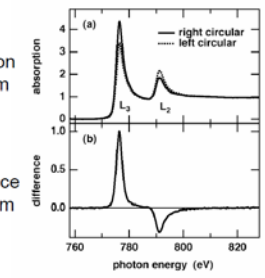

XMCD difference spectrum for different limiting cases

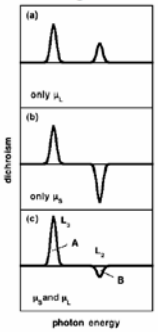

From: X-ray magnetic circular dichroism for quantitative element-resolved magnetic microscopy, by Wolfgang Kuch

Hercules Sept 2015

Science & Technology Facilities Council ISIS

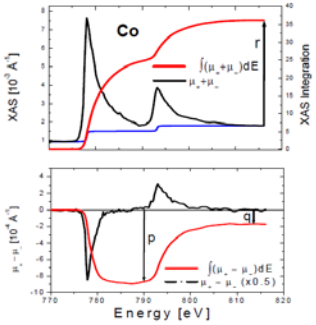

Sum rules according to Thole and Carra, neglecting dipole terms:

$$m_{orb}[\mu_B/\text{atom}] = -\frac{4qh}{3r}$$

$$m_{spin}[\mu_B/\text{atom}] = -\frac{(6p-4q)h}{r}$$

$$\Rightarrow \frac{m_{orb}}{m_{spin}} = \frac{2q}{9p-6q}$$

$$h = (10-3d)$$

B.T. Thole, P. Carra, F. Sette, G. van der Laan, PRL 68 (1992) 1943; PRL 70 (1993) 694

Courtesy: H . Zabel

Hercules Sept 2015

Science & Technology Facilities Council ISIS

Photon-In Electron-Out

- 3 Selectivities

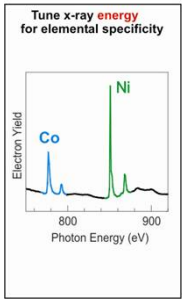

J. Stöhr (2006)

Hercules Sept 2015

Science & Technology Facilities Council ISIS

XRMS

$$f = f_0 + f' + if'' + f_{Spin}$$

$$f^{Mag}_{Non-res} = ir_0(\hbar\omega)f_D[\frac{1}{2}\vec{L}(\vec{Q})\cdot\vec{A} + \vec{S}(\vec{Q})\cdot\vec{B}]$$

$$F^e_{LM}(\omega) = \sum_{\alpha,\eta}(P_\alpha P_\alpha(\eta)\Gamma_x(\alpha M\eta; EL)/\Gamma(\eta))/(x(\alpha,\eta) - i)$$

$$f^{XRES}_{nE1} = ((\hat{\epsilon}'\cdot\hat{\epsilon})F^0 - i(\hat{\epsilon}'\times\hat{\epsilon})\cdot\hat{z}_n F^1 + (\hat{\epsilon}'\cdot\hat{z}_n)(\hat{\epsilon}\cdot\hat{z}_n)F^2)$$

$$F^0 = \frac{3}{4k}[F_{11} + F_{1-1}]$$

$$F^1 = \frac{3}{4k}[F_{11} - F_{1-1}]$$

$$F^2 = \frac{3}{4k}[2F_{10} - F_{11} - F_{1-1}]$$

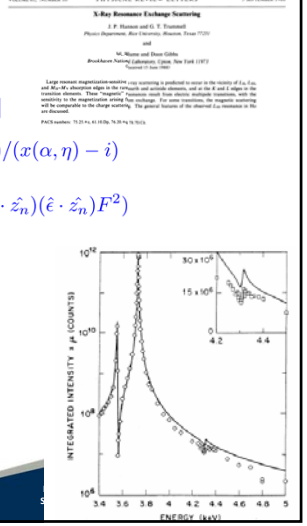

- Namikawa *et al.* 1985 NiO
- McWhan *et al* 1990 UAs
- Hill and McMorrow Acta Cryst. (1996). **A52**, 236-244

Refractive Index

$$n = \frac{c}{v}$$

- *n* varies with wavelength: dispersion

$$n_1 \sin\theta_1 = n_2 \sin\theta_2$$

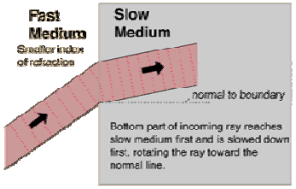

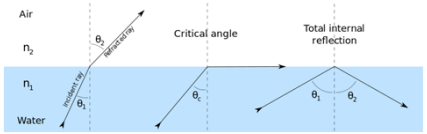

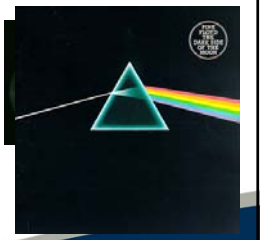

http://hyperphysics.phy-astr.gsu.edu
en.wikipedia.org

Hercules Sept 2015 — Science & Technology Facilities Council ISIS

$$n = 1 - \lambda^2 A - i\lambda B \quad (1)$$
$$A = \frac{Nb}{2\pi} \quad (2)$$
$$B = \frac{N(\sigma_a + \sigma_i)}{4\pi} \quad (3)$$
$$n = 1 - \alpha - i\beta \quad (1)$$
$$\alpha = \frac{N\lambda^2 |r_e}{2\pi} \quad (2)$$
$$\beta = \frac{\lambda\mu}{4\pi} \quad (3)$$

n <1 Total External reflection

Index of Refraction: Neutrons

$$n = \frac{\sin\gamma_i}{\sin\gamma_t} = \frac{|\vec{k_t}|}{|\vec{k_i}|}$$

$$n^2 = \frac{|\vec{k_t}|^2}{|\vec{k_i}|^2} = \frac{E_t}{E_i} = \frac{E_i - V_n}{E_i} = 1 - \frac{4\pi}{k_i^2} Nb$$

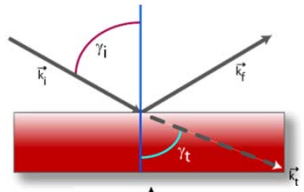

$$V_n = \frac{2\pi\hbar^2}{m_n} Nb$$

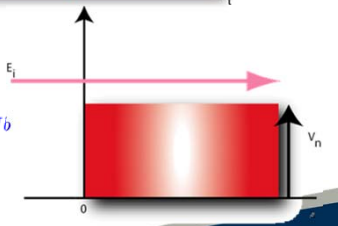

Hercules Sept 2015 — Science & Technology Facilities Council ISIS

Critical Reflection

- $\frac{\cos\alpha_i}{\cos\alpha_f} = \frac{n_2}{n_1}$
- At the critical angle $\frac{\cos\alpha_i}{\cos 0} = n$

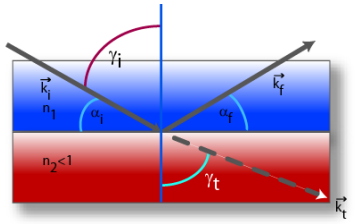

$$Q_c = \frac{4\pi}{\lambda} 2k\sin\alpha_c = 2k\sqrt{1-\cos^2\alpha_c} = \sqrt{4k^2\left(1-n^2\right)} \cong \sqrt{4k^2 \cdot 2\delta} = \sqrt{16\pi Nb}$$

Material	θ_c / Å
Ni	0.1
Cu	0.083
Al	0.047
Si	0.047
D_2O	0.082

- Q_c only depends on the material!

Hercules Sept 2015 — Science & Technology Facilities Council ISIS

Index of Refraction: Photons

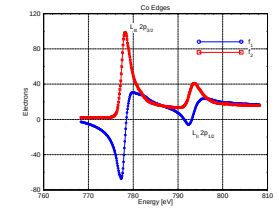

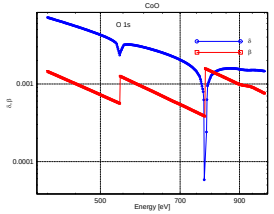

$$
\begin{aligned}
n &= 1-\delta-i\beta \\
&= 1-\frac{r_e}{2\pi}\lambda^2\sum_i n_i f_i(0) \\
f(0) &= f_1+if_2 \\
&= f_1+i\frac{\sigma_a}{2r_e\lambda} \\
&= Z^*+\frac{1}{\pi r_e hc}\int_0^\infty \frac{\epsilon^2\sigma_a(\epsilon)}{E^2-\epsilon^2}
\end{aligned}
$$

http://www-cxro.lbl.gov/optical_constants/

Specular Scattering

Neutron and x-ray reflectivity

How do we connect the scattering length profile with the reflectivity

Using the neutron's spin

- The neutron is a spin ½ particle
- The neutron possesses an intrinsic magnetic moment: spin
- Caution…

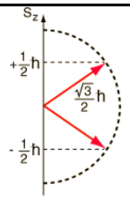

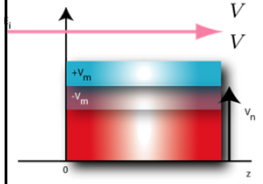

Nuclear Magnetic

$$
\begin{aligned}
V &= V_n+V_m && (1)\\
V &= \frac{\hbar}{2\pi m}Nb \quad -\mu\cdot\mathbf{B} && (2)\\
&= -4\pi\mu_n\cdot M && (3)\\
&= -\frac{2\hbar\pi^2}{m_n}p(z)\sin(\theta) && (4)\\
&= \frac{2\hbar\pi^2}{m_n}\frac{M_p}{M_s}N\frac{m_n\mu_n\mu_0}{2\pi\hbar^2}\mu_s && (5)
\end{aligned}
$$

$$
\vec{\mu_n}=\gamma\mu_N\vec{\sigma}
$$

$$
\sigma_x=\begin{pmatrix}0&1\\1&0\end{pmatrix},\sigma_y=\begin{pmatrix}0&-i\\i&0\end{pmatrix},\sigma_z=\begin{pmatrix}1&0\\0&-1\end{pmatrix}
$$

Fresnel's law for a surface and thin film

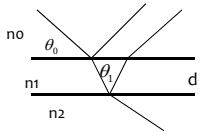

$$
k_i=n_i\sin\theta
$$

$$
\beta_i=\frac{2\pi}{\lambda}n_i d_i\sin\theta_i
$$

$$
R(Q)=\left|\frac{r_{01}+r_{12}\exp(-2i\beta_i)}{1+r_{01}r_{12}\exp(-2i\beta_i)}\right|^2
$$

$$
r_{ij}=\frac{a_r}{a_i}=\frac{k_i-k_j}{k_i+k_j}
$$

$$
t_{ij}=\frac{a_j}{a_i}=\frac{2k_i}{k_i+k_j}
$$

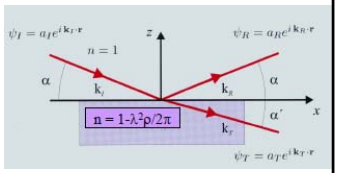

http://www.che.udel.edu/cns/pdf/Reflectometry.pdf

PNR from a single layer

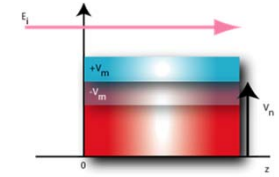

$$V = V_n + V_m \quad (1)$$

$$V = \frac{\hbar}{2\pi m} N(b \pm p) \quad (2)$$

$$p = (2.695 \times 10^{-4}/\mu_B)\,|\vec{\mu}_i|$$

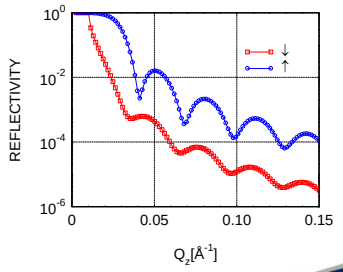

Parratt Iteration

Surface Studies of Solids by Total Reflection of X-Rays*

L. G. Parratt

Cornell University, Ithaca, New York

(Received March 22, 1954)

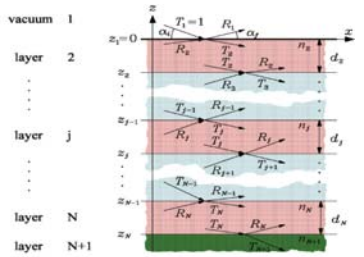

$$X_j = \frac{R_j}{T_j} = \exp(-2ik_{z,j}z_j)\frac{r_{j,j+1} + X_{j+1}\exp(2ik_{z,j+1}z_j)}{1 + r_{j,j+1}X_{j+1}\exp(2ik_{z,j+1}z_j)}$$

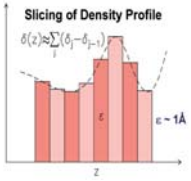

Can now simulate profile with a "*slice and dice*" approach

PNR from a multiple layers

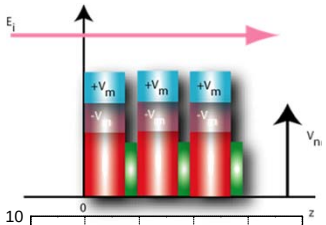

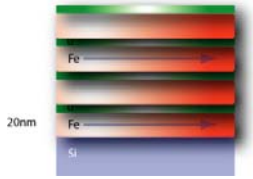

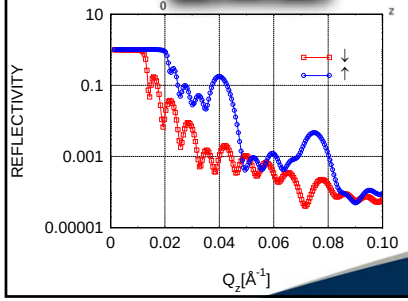

Spin dependent cross-section

- In-plane orientation of magnetisation obtainable from 4 spin dependent cross-sections

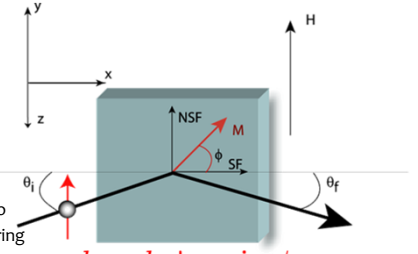

- Components of the magnetisation, m give rise to
- m | | H: Non Spin Flip Scattering (NSF)
- m ⊥H: Spin Flip Scattering (SF)
- Dynamical analysis gives absolute depth dependence profile

$$b = b + p\sin\phi$$

$$p_m \cos\phi = p_x$$

$$\left[\frac{-\hbar^2}{2m_n}\nabla^2 + V(r)\right]\Psi^{\uparrow,\downarrow} = E\Psi^{\uparrow,\downarrow}$$

Polarisation

Polarised neutron reflection

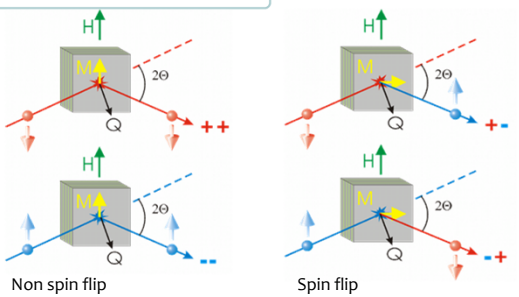

Non spin flip
++ measures b + M_z
- - measures b - M_z

Spin flip
+ - measures M_x + iM_y
- + measures M_x - iM_y

By fitting all components the direction and strength of the magnetic moment can be measured as a function of depth

Science & Technology Facilities Council ISIS

Polarisation

Polarising supermirrors

Magnetic materials have a spin dependent term in their refractive index

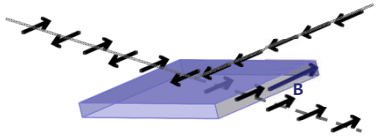

An ~60%/40% Fe/Co mirror works well at saturation

Science & Technology Facilities Council ISIS

Caveat to Classical Description

- CD predicts a continous variation of critical edge

$$\frac{4\pi \sin(\alpha_c^{\pm})}{\lambda} = Q_c^{\pm} = \sqrt{\frac{2m_n}{\hbar^2}(V_n \pm |\mu|\,|B_s|\cos(\theta))}$$

- Stern-Gerlach effect? Only 2 eigenstates

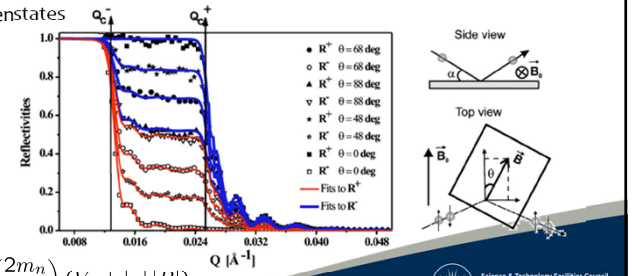

$$k_{\pm}^2 = \left(\frac{2m_n}{\hbar^2}\right)(V_n \pm |\mu|\,|B|)$$

Science & Technology Facilities Council ISIS

Roughness

Structural and magnetic interfacial phenomena

Science & Technology Facilities Council ISIS

Structural Roughness

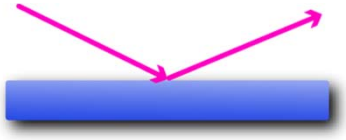

$$R(Q) = R_F \exp\left(-Q^2\sigma^2\right)$$

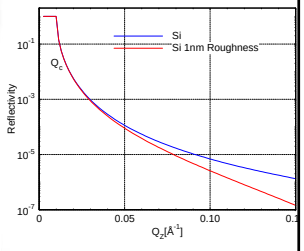

PHYSICAL REVIEW B VOLUME 38, NUMBER 4 1 AUGUST 1988

X-ray and neutron scattering from rough surfaces

S. K. Sinha, E. B. Sirota, and S. Garoff*
Corporate Research Science Laboratory, Exxon Research and Engineering Company, Clinton Township, Route 22 East, Annandale, New Jersey 08801

H. B. Stanley†
University of Maryland, College Park, Maryland 20742
(Received 30 November 1987)

$$C(R) = \left\langle \left[z(x,y) - z(x',y') \right]^2 \right\rangle = \sigma^2 \exp(-r/\xi)^{2h}$$

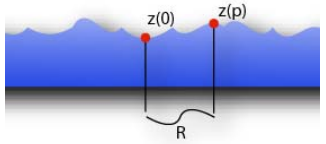

- σ= roughness
- ξ= cut-off length:
  - for R > ξ, interface appears smooth,
  - for R < ξ, interface appears rough, fractal behaviour
- h=3-D Hurst parameter for jaggedness(0<h<1)
  - smooth: D=2, h=1
  - very rough D=3, h=0

Simulation Packages

Simulation Packages: neutron

http://neutronreflectivity.neutron-eu.net/main/SimulationPrograms

Simulation Packages: photon

- X-ray
  - http://sergey.gmca.aps.anl.gov/
  - ESRF
  - RefTool
  - GenX

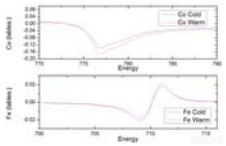

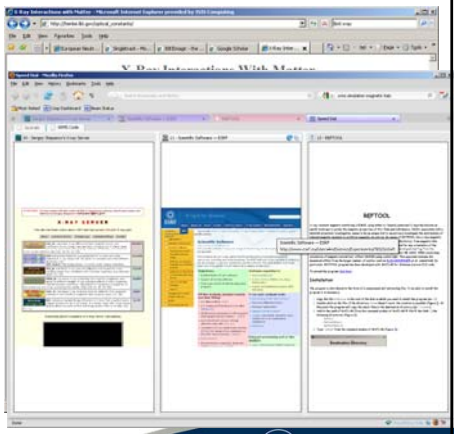

GenX (neutron and x-ray reflectivity)

- Sourceforge

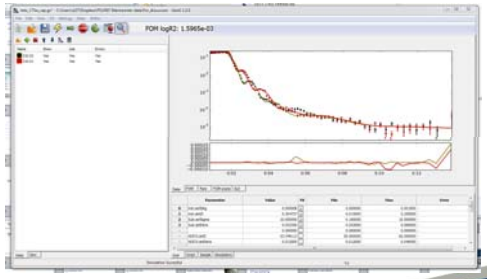

Off-specular scattering

Probing in-plane lengthscales

L_{Coh}<Domain size

- $I \propto \sum_i \left(A_i^2\right)$
- Only specular scattering

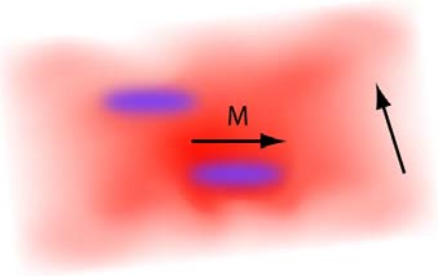

L_{Coh}>Domain size

$I \propto (\sum_i A_i)^2$

- Only diffuse scattering

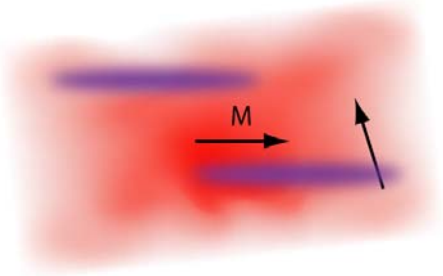

Experimental Geometry

- λ range 0.5-6.5Å
- 1-d Detector
- Typical acquisition~2hours/field
- Measured coherence length ~30μm

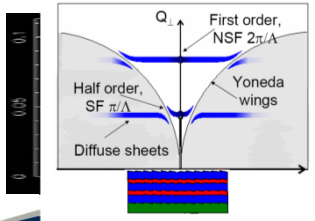

Diffuse scattering

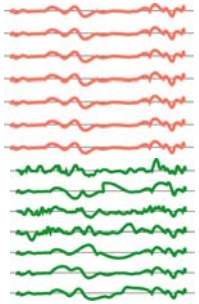

Holý and Baumbach, prb, 49, 10668, (1994)

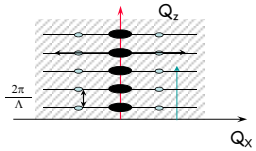

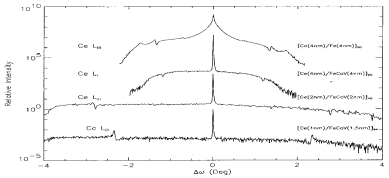

(Ce/Fe) Tixier, Mannix et al.

Kinematic calculation

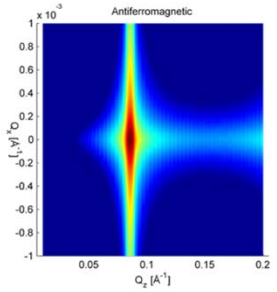

- Langridge *et al. Phys. Rev. Lett.* (2000) **85,** 4964

Coercive Field $\theta = \frac{Q_z}{2Q_i} - \frac{Q_x}{2Q_z}$

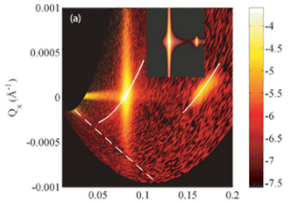

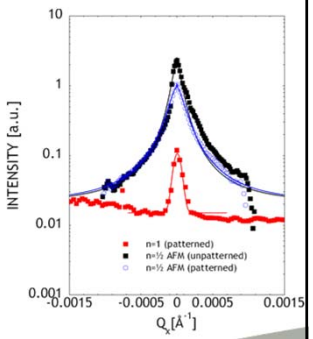

AFM FM

Domains and the coherence volume

Many thanks to H. Zabel for slides

Domain size: 100 μm (> L_c)

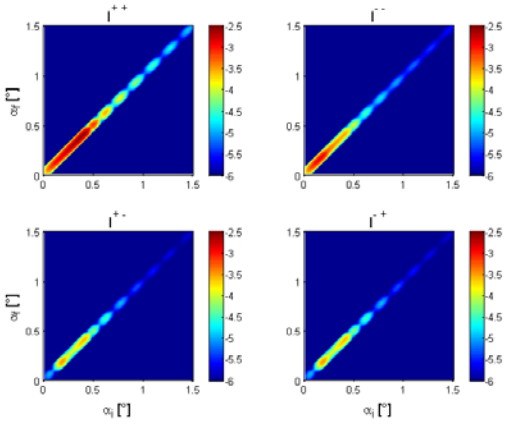

Domain size: 100 μm

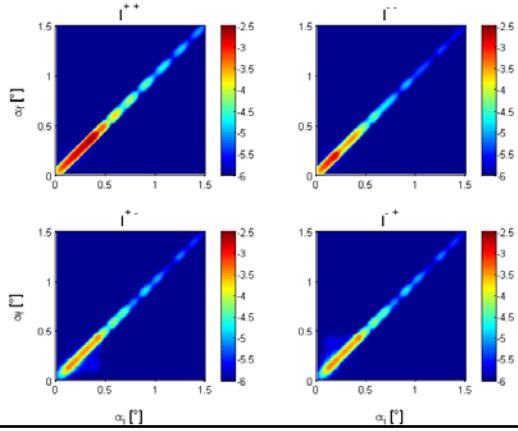

Domain size: 50 μm

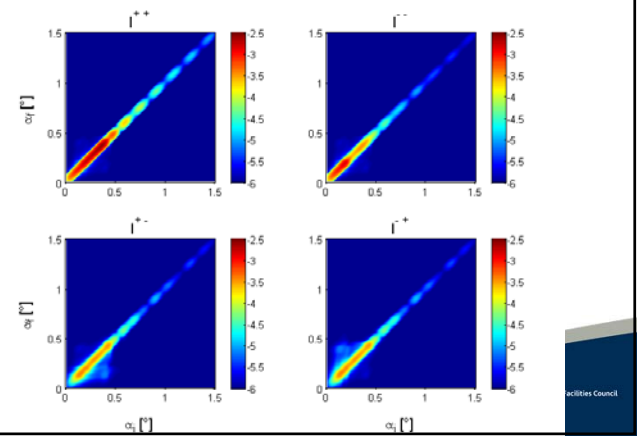

Domain size: 10 μm

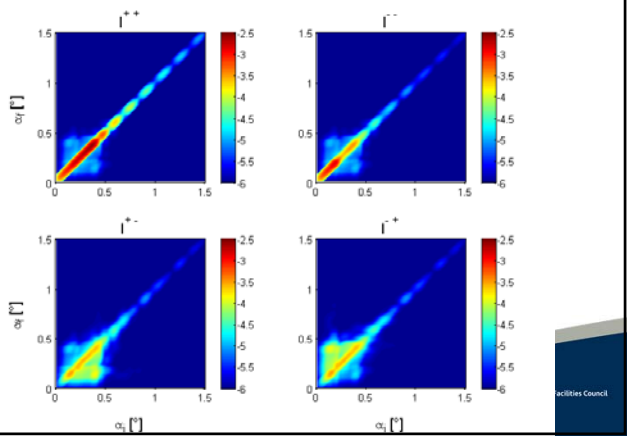

Domain size: 5 μm

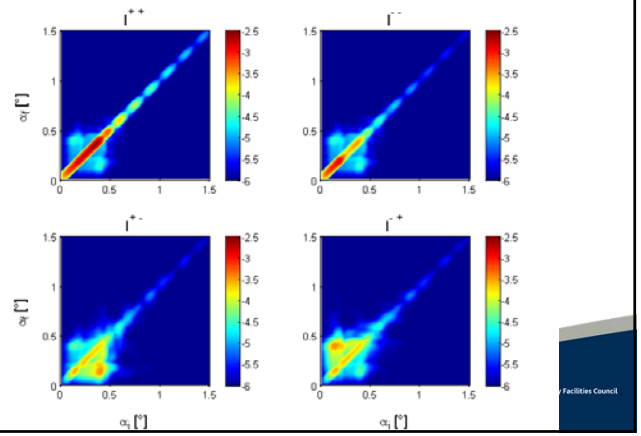

Domain size: 1 μm

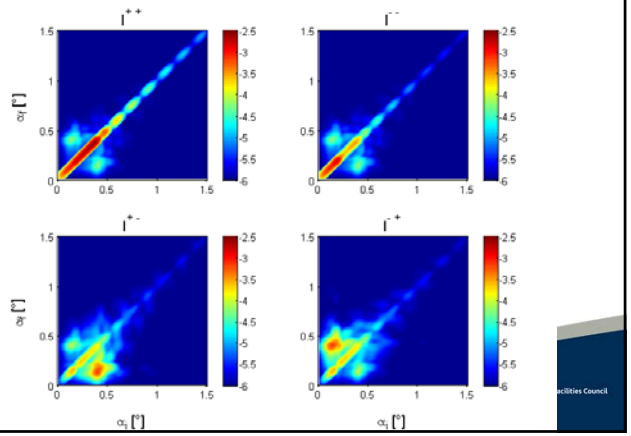

Single ferromagnetic film in the domain state

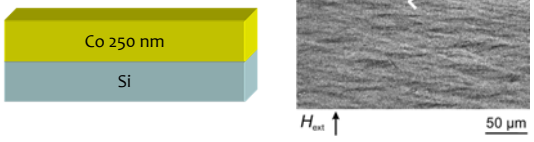

F. Radu *et al*, J. Phys.: Condens. Matter **17** (2005) 1711-1718

Banana shape off-specular scattering from domain state

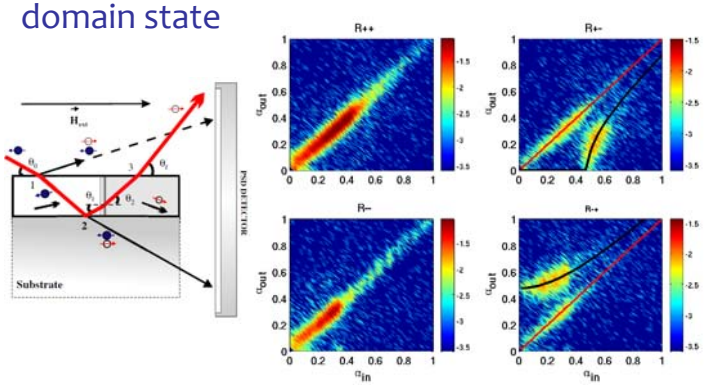

Simulation of domain state

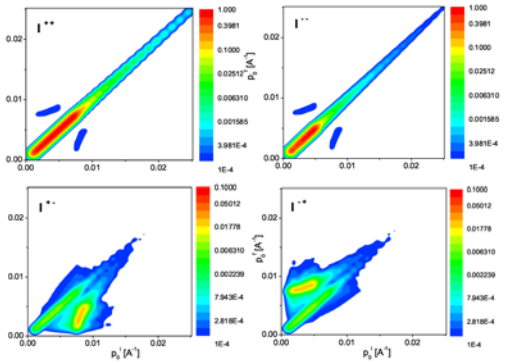

B.P. Toperverg Physica B **297** (2001) 160-168

XPEEM: X-ray Photoelectron Emission Microscopy

- Spatial resolution ~ 30 nm
- Short acquisition times
- Element sensitive technique (XMC(L)D)
- Surface sensitive technique
- Real Space Technique

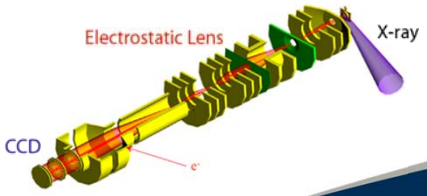

http://www.diamond.ac.uk

Imaging Interfacial Magnetism

- Mixed layer

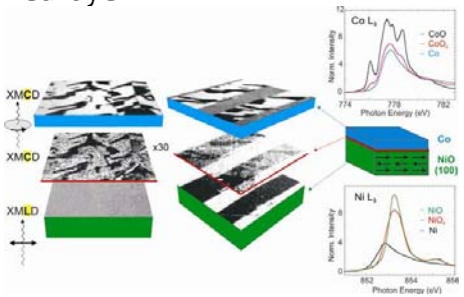

H. Ohldag, *et al* Phys. Rev. Lett. 87, 7201 (2001)

http://www-ssrl.slac.stanford.edu/stohr/magneticexchange.htm

Soft x-ray beamline i06/i10

i06	diamond
Energy range (first harmonic circular) (eV)	106 - 1300
Energy range (linear horizontal) (eV)	80 - 2100
Energy range (linear vertical) (eV)	130 - 1500
Resolving power (Δ E/E)	10,000 @ 400eV
Spot size at PEEM (μm) (FWHM)	10 (H) x 3 (V)
Spot size on sample surface (μm)	ϕ = 10

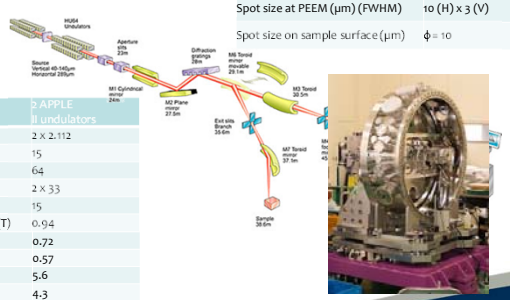

Insertion device	2 APPLE II undulators
Nominal magnet length (m)	2 x 2.112
Nominal magnet gap (mm)	15
Magnet period (mm)	64
Number of periods	2 x 33
Nominal magnet gap (mm)	15
Peak field in horizontal mode (T)	0.94
Peak field in vertical mode (T)	0.72
Peak field in circular mode (T)	0.57
K_{MAX} in horizontal mode	5.6
K_{MAX} in vertical mode	4.3
K_{MAX} in circular mode	3.4

Reflectometers

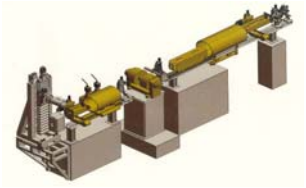

- Continuous or tof mode of operation
- 5Å Monochromator (6Å Polarised)
- White beam flux 9.6x10^9 n/s/cm^2

- The CRISP reflectometer at ISIS is a white beam time of flight (tof) polarised neutron reflectometer viewing a 20K hydrogen moderator.

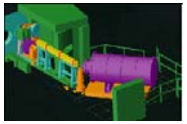

http://www.ill.fr/YellowBook/D17/

http://www.ill.fr/YellowBook/ADAM/

PolRef

- Waveler
- Unpolar
- Polarize

- Source t
- Beam in

- Well shi
- 640 channel linear gas detector with 0.5mm pixel

- Vertical 2θ 7.5°
- Horizontal 2θ 22°

Polref schematic

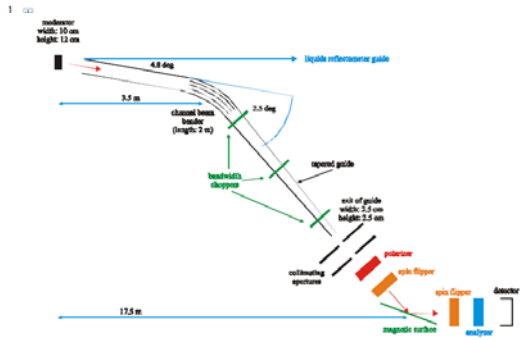

Figure 1 An outline side schematic of polREF.

Examples of reflectivity

Quantum Well State

- Band matching important *e.g.* Fe/Cr

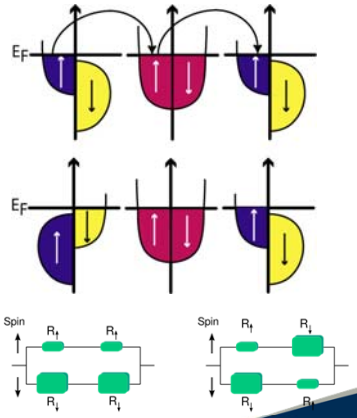

Co/Cu GMR

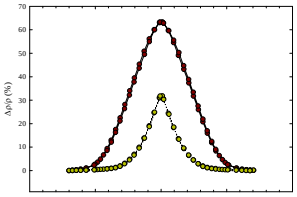

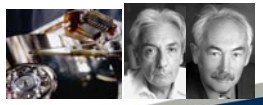

Real space Imaging of IEC

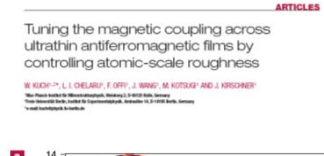

ARTICLES

Tuning the magnetic coupling across ultrathin antiferromagnetic films by controlling atomic-scale roughness

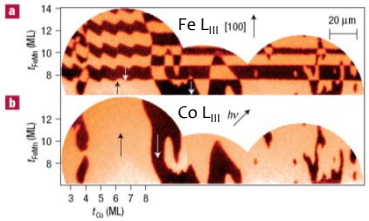

- Crossed Wedge
  - Co(001)/Co/FeMn/FeNi
  - Regions of parallel and anti-parallel coupling
  - Sawtooth Oscillation
  - 2ML period IEC

Spin Accumulation

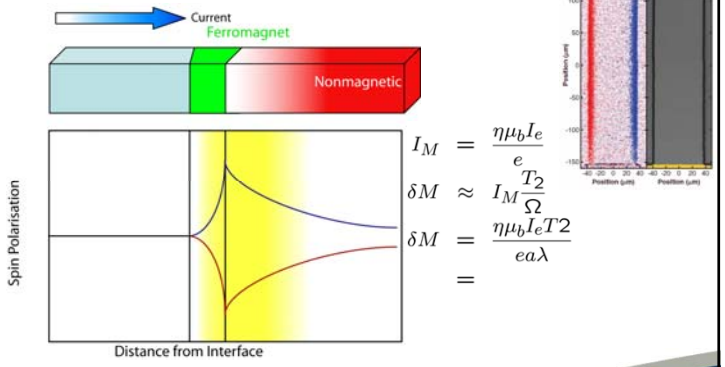

$$I_M = \frac{\eta \mu_b I e}{e}$$

$$\delta M \approx I_M \frac{T_2}{\Omega}$$

$$\delta M = \frac{\eta \mu_b I_e T 2}{e a \lambda}$$

$$=$$

- A. Fert *et al.*, *J. Phys. D: Appl. Phys.* **35** (2002) 2443-2447
- M. Johnson and R.H. Silsbee *Phys. Rev. Let.* **55** (1985) 1790
- Kato *et al.* Science **306** 1910 (2004)

Structural Characterisation

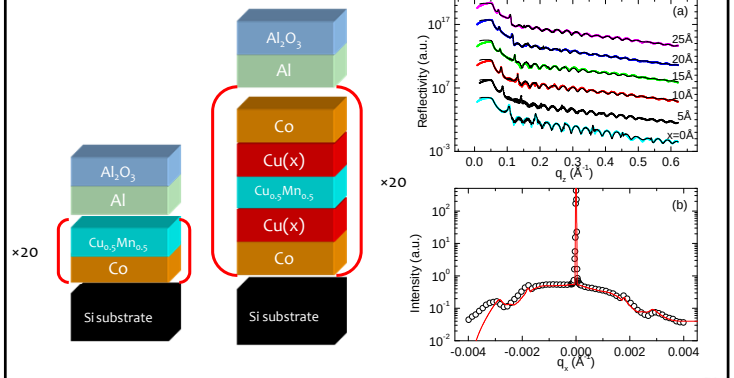

TABLE I. Best fit parameters for the specular reflectivity of the Co/Cu1(*x*)/CuMn/Cu2(*x*) multilayers.

	Thickness				Interface Morphology			
x	Co ±1Å	Cu1 ±0.5Å	CuMn ±0.5Å	Cu2 ±0.5Å	$\sigma_{topological}$ ±0.5Å	$\sigma_{grading}$ ±0.5Å	ξ ±20Å	h ±0.1
0	42	-	23.5	-	5.5	1.0	140	0.5
5	41	6.5	22.5	5.5	4.0	0.5	170	0.5
10	41	12.0	19.5	11.5	5.0	1.0	220	0.5
15	43	16.5	23.0	17.5	5.5	0.5	180	0.5
20	39	22.5	20	21.0	5.5	0.5	180	0.5
25	43	27.0	22.5	28.5	6.0	1.0	250	0.5

Optical constants

- Obtained from XAS and XMCD
- Co 1.5$\mu_{B\ spin}$ 0.21 $\mu_{B\ Orbital}$

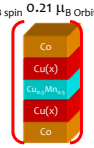

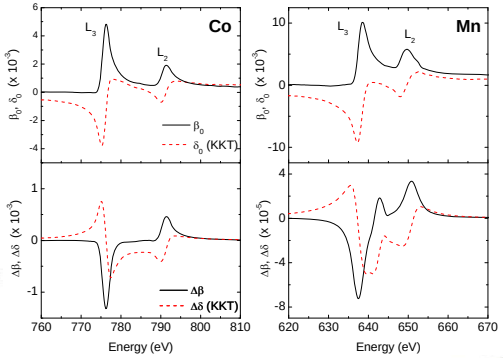

$$\delta^{\pm} = \left(\frac{2\pi n_0 r_e}{k^2}\right)\left[f_0 + f'(E) \mp m'(E)\cos\theta\right]$$

$$\beta^{\pm} = \left(\frac{2\pi n_0 r_e}{k^2}\right)\left[f''(E) \mp m''(E)\cos\theta\right]$$

$$\delta^{\pm} = \delta_0 \mp \Delta\delta$$

$$\beta^{\pm} = \beta_0 \mp \Delta\beta$$

$$n_j^{\pm} = 1 - \delta_j^{\pm} + i\beta_j^{\pm}$$

Hysteresis Loops

- Comparison of Co and Mn
- Clear transition from ⇅ to ⇈
- Mn rotates with the Co

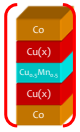

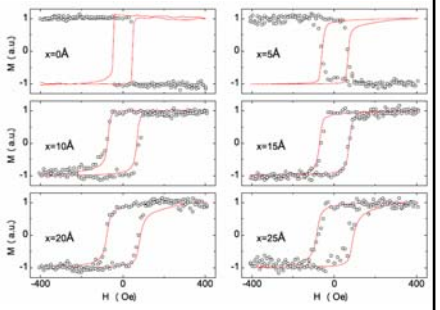

- E=780eV
- Circular polarization

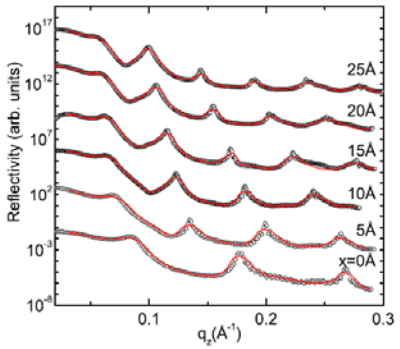

Cu

- Decays sharply away from the interface
- Agreement with previous measurement

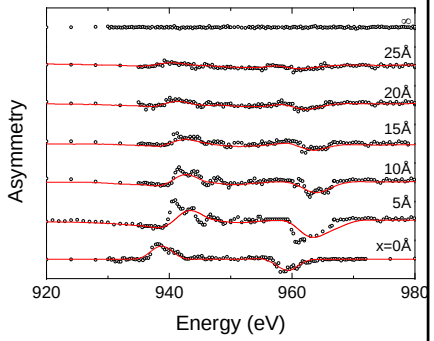

Mn dichroism

- Large effect
- Decaying away from interface

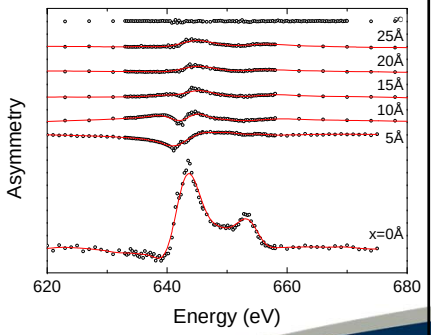

Magnetisation Profile in the Cu/Mn

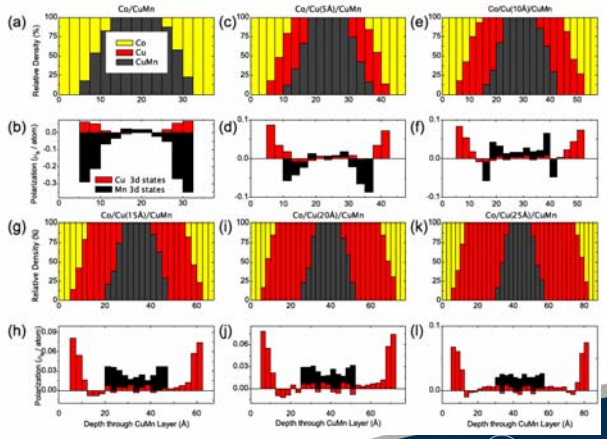

DFT-DOS

- Supercell 4 atoms of Cu and Mn
  - 0.05μ_B on Cu *d* orbital
  - Decays rapidly from interface

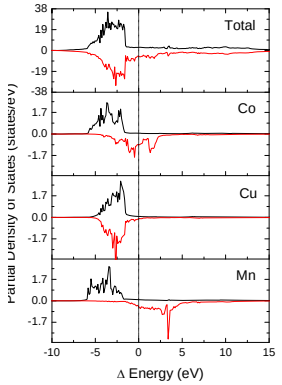

Quantum Oscillations

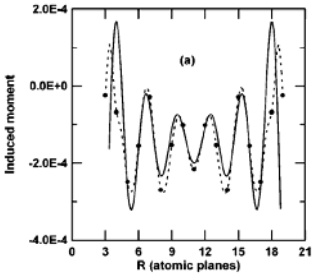

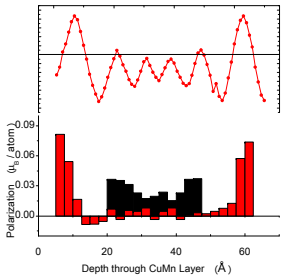

- Mathon *et al.* PRB **59** 6344 (1999)

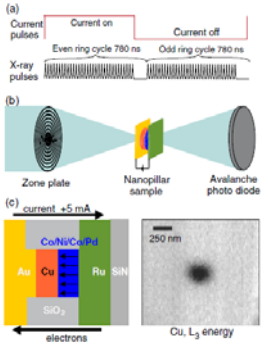

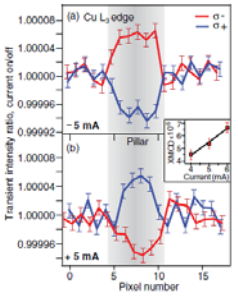

Kukreja R *et al.* X-ray Detection of Transient Magnetic Moments Induced by a Spin Current in Cu *Phys. Rev. Lett.* **115** 096601 (2015)

A Controllable Magnetic Interface

Motivation

- Tuneable Magnetostructural phase transition
  - J.S. Kouvel, C.C. Hartelius, J. Appl. Phys., **33**, 1343 (1962)
  - L. Zsoldos, Phys. Stat. Sol., **20**, K25 (1967)
  - Anomalously strong electron-lattice coupling
  - Fundamental interest experimentally and theoretically
    - Nature of the stability of the FM phase
    - Kudrnovský, J.*et al. Phys. Rev.* B **91,** 014435 (2015)

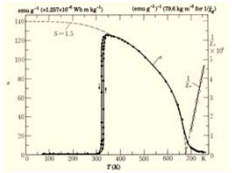

- Ultra-fast switching
  - Ju *et al.* Phys. Rev. Lett. **93,** 197403 (2004)
  - Radu *et al.* prb **81,** 104415 (2010)
  - Quirin *et al.* prb **85,** 020103(R) (2012)
- Ability to control through heterostructure design
- Spintronic Applications
  - Marti, X. *et al.*. *Nat. Mater.* **13,** 367 (2014)
  - Naito, T. *et al. J Appl Phys* **109,** 07C911 (2011)

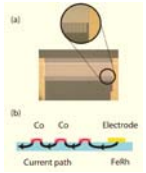

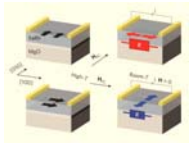

- HAMR, magnetic refrigeration
  - FePt/FeRh system
    - Thiele *et al.* Appl. Phys. Lett. **82** 2859 (2003)
  - Control MTJ cell coercivity

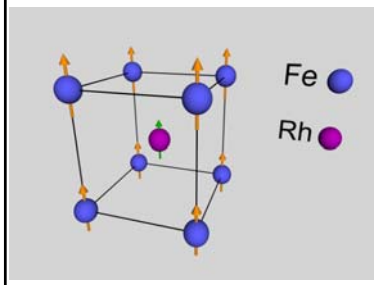

- CsCl structure
  - a~2.99Å
  - α' phase
- 300K: Type G AF
- Fe: ~3.3 μ_B
- Rh: no moment
- FM alignment within <111> planes
- AF alignment between <111> planes
- 350 K: AF → FM
- Fe: ~3.1 μ_B
- Rh: ~1 μ_B

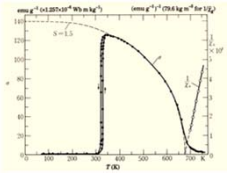

- J. S. Kouvel and C. C. Hartelius, JAP, **33,** 1343 (1962).
- G. Shirane *et al.* Phys. Rev. **134,** A1547 (1964)

Strain and Pd doping

- Transition temperature is tuneable via doping and field
  - T_{AF-F} can be increased by doping with Ir and Pt and decreased by doping with Pd and Ni.
  - Shift to lower temperatures observed by application of applied field.

- P. Kushwaha, A. Lakhani, R. Rawat, and P. Chaddah, Physical Review B **80,** (2009)

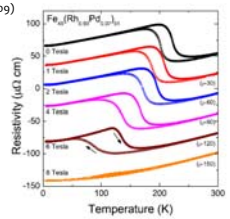

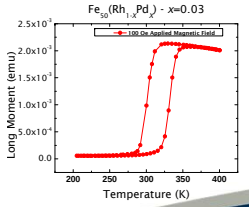

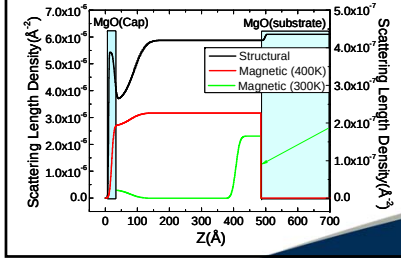

Sample Growth

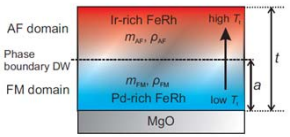

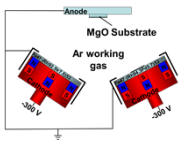

- Base pressure: ~5·10^{-8} torr.
- Sputtered using two angled DC magnetrons.
- Alloy targets used to make $FeRh_{1-x-y}Pd_xIr_y$:
  - Fe47(Rh92.5Ir7.5)53
  - Fe47(Rh94.3Pd5.7)53
- Substrate: MgO(001)
- Nominal FeRh(Pd/Ir) thickness 50nm.
- Post-growth anneal at 600˚C for 60 min.
- Al (3nm) Cap deposited at 100˚C.
- Aim is for anneal to diffuse layers for smooth doping gradient.

- Transition controllable by:
  - Temperature
  - Field (H)
  - Doping – Pd, Pt (decrease T_t) or Ir, Ni (increase T_t)
  - Strain - R. Fan, *et. al.* Phys Rev B 82, 184418 (2010)
  - Pressure – S. Yuasa *et. al.* Phys. Soc. Jap. 63, 3, 855-858(1994).
  - Ion Beam -- Koide, T. *et al. J. Appl. Phys.* **117,** 17E503 (2015).
- Possible to create a controllable magnetic interface via a doping gradient

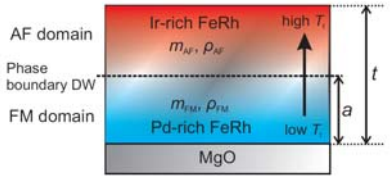

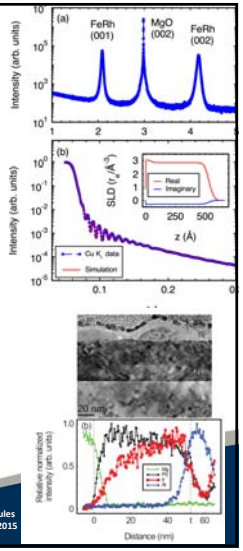

- Basis for a field or temperature sensor

Magnetisation measurements

- Phenomenological characterisation of the FM phase

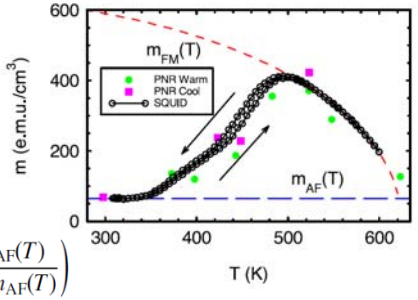

$$a(T) = t\left(\frac{m(T) - m_{\mathrm{AF}}(T)}{m_{\mathrm{FM}}(T) - m_{\mathrm{AF}}(T)}\right)$$

Resistance measurements

- Large change in carrier density across the transition

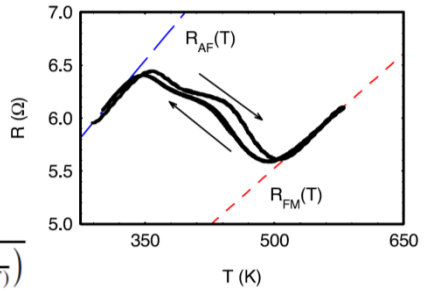

$$a(T) = t\frac{\left(1 - \frac{R(T)}{R_{\mathrm{AF}}(T)}\right)}{\left(\frac{R(T)}{R_{\mathrm{FM}}(T)} - \frac{R(T)}{R_{\mathrm{AF}}(T)}\right)}$$

de Vries, M. A. *et al.* Hall-effect characterization of the metamagnetic transition in FeRh. *New J. Phys.* **15,** 13008 (2013).

Neutron Measurements

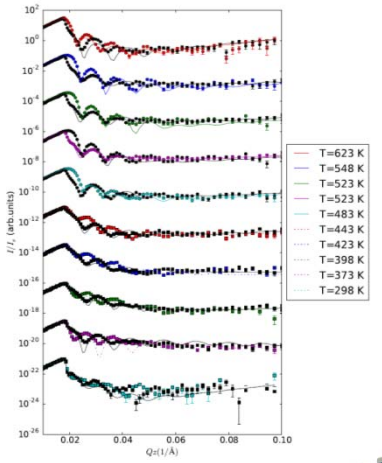

- Saturating Field
- Constrained two layer model
  - The minimum to describe the data

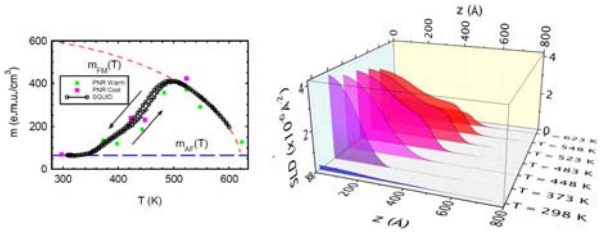

- Evidence of a controllable, mobile magnetic (electronic) domain wall
- Complex structure
- Neutrons essential to quantitatively resolving the complex magnetic structure

Le Graët, C. *et al.* Temperature controlled motion of an antiferromagnet- ferromagnet interface within a dopant-graded FeRh epilayer. *APL Mater.* **3,** 041802 (2015)

Summary & Outlook

- We have produced a controllable magnetic(electronic) domain wall in a heterostructure
- Provided a nanoscale description which is quantitatively consistent with macroscopic measurements
- The tunability of this system presents a fascinating playground for basic research and for potential device and sensor applications

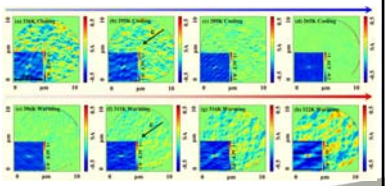

Le Graët, C. *et al.* Temperature controlled motion of an antiferromagnet- ferromagnet interface within a dopant-graded FeRh epilayer. *APL Mater.* **3,** 041802 (2015).
Kinane, C. J. *et al.* Observation of a temperature dependent asymmetry in the domain structure of a Pd-doped FeRh epilayer. *New J. Phys.* **16,** 113073 (2014).

Superconductivity and reflectivity

Towards superconducting spintronics

Flux penetration in superconductors

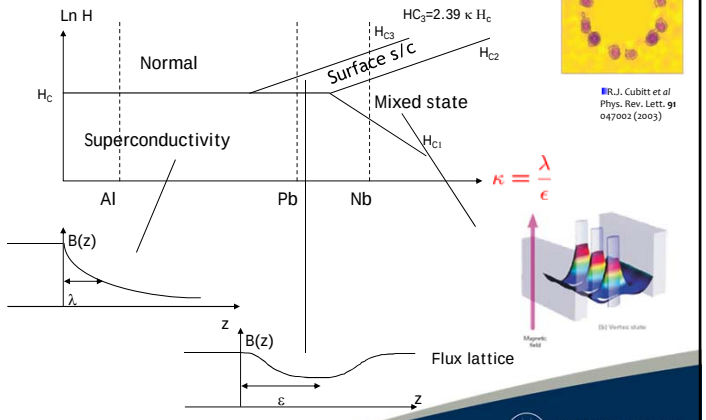

R.J. Cubitt *et al* Phys. Rev. Lett. **91** 047002 (2003)

Flux penetration in superconductors

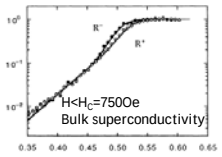

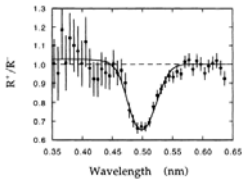

FIG. 2. The spin-dependent reflectivities R^+ and R^- measured in an applied magnetic field of 6.0×10^4 A/m (750 Oe). The continuous lines are the reflectivities calculated for the two polarization states, with the same instrumental and surface parameters as in Fig. 1, and an exponential decay of magnetic induction with a penetration depth of 39 nm.

PHYSICAL REVIEW B VOLUME 49, NUMBER 22 1 JUNE 1994-II

Magnetic-induction profile in a type-I superconductor by polarized-neutron reflectometry

M. P. Nutley*
Institut Laue-Langevin, 156X, 38042 Grenoble CEDEX, France

A. T. Boothroyd and C. R. Staddon
Department of Physics, Clarendon Laboratory, University of Oxford, Parks Road, Oxford, OX1 3PU, United Kingdom

D. M°K. Paul
Department of Physics, University of Warwick, Coventry, CV4 7AL, United Kingdom

J. Penfold
ISIS Science Division, Rutherford Appleton Laboratory, Chilton, Didcot, Oxon., OX11 0QX, United Kingdom

(Received 17 February 1994)

- 1μm Pb film
- PbO surface layer
- $B(z)=\mu_0 H \exp(-z/\lambda)$
- $\lambda=39\pm1$nm
- No field dependence

Science & Technology Facilities Council ISIS

Visualising the Flux distribution

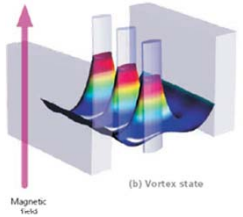

$d = 195nm$

$d = 250nm$

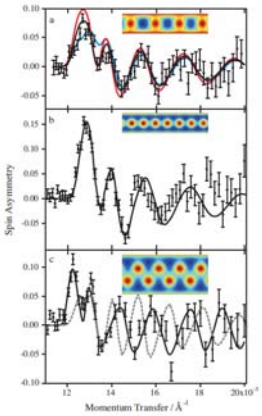

A Drew *et al* Phys. Rev. B. **80** 134510 (2009)

Science & Technology Facilities Council ISIS

Generating a triplet state

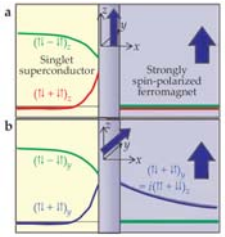

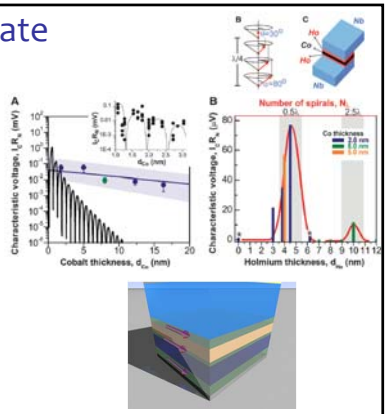

- first found in heavy fermion materials such as UGe_2 or URhGe
- *orbital* and *spin* components of the wavefunction are both *even* with respect to electron exchange, thus they must be an *odd-frequency*; odd with respect to time reversal
- non-collinear magnetism within a distance of the coherence length required

- Robinson *et al. Science* **329**, 59 (2010)
- Banerjee *et al.* Nat. Commun. **5**, 1 (2014).
- M. Eschrig Physics Today (2011)

Science & Technology Facilities Council ISIS

Generating a triplet state

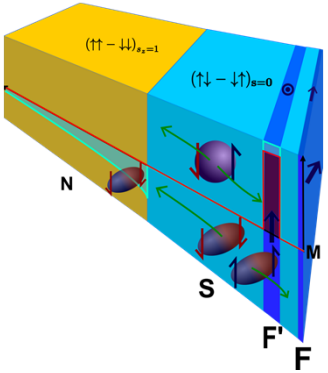

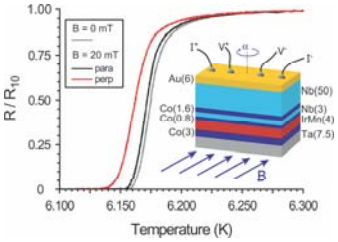

- F. S. Bergeret, A. F. Volkov, and K. B. Efetov, Rev. Mod. Phys. **77**, 1321 (2005)
- M. G. Flokstra, **CJK, JFKC, SL**, *et al.* Phys. Rev. B **060501(R)**, (2015)

Science & Technology Facilities Council ISIS

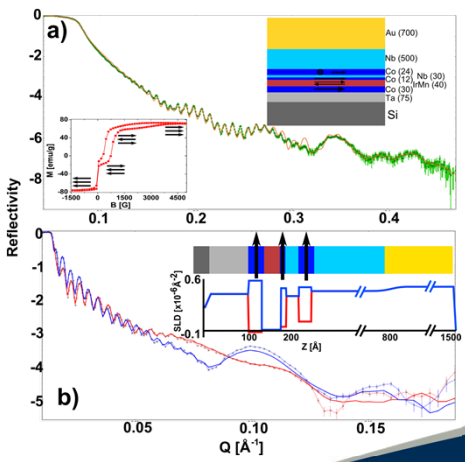

- Combined neutron and x-ray characterisation
- High Quality samples
  - Break down the structure and rebuild the analysis

- Negative moment in the Au layer
- ~0.1μ_b change in Co

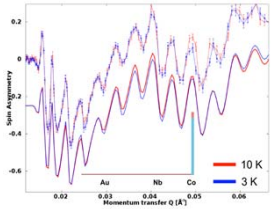

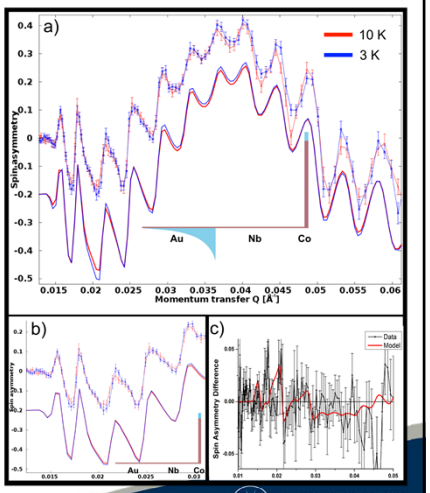

M. G. Flokstra, **CJK, JFKC, SL,** *et al.* Phys. Rev. B **060501(R)**, (2015)

Remotely Induced Magnetism from a superconducting spin valve

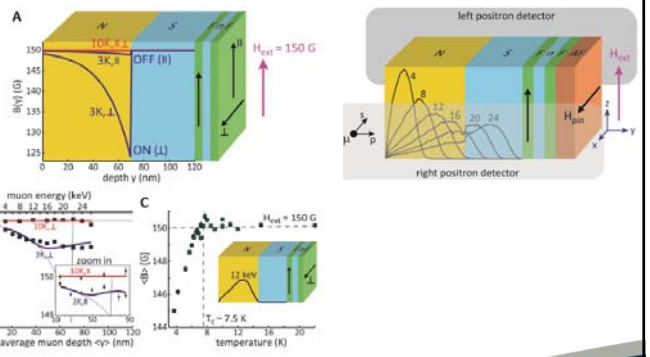

M. G. Flokstra, **CJK, JFKC, SL,** *et al.* arXiv:1505.03565 (2015) In press

PNR Summary

- Length scale of induced magnetisation too long for inverse proximity.
  - Flokstra PRB 89 054510
- Profile is not the parabola shape expected for Meissner screening.
  - Khaydukov arXiv:1405.0242
- Induced moment in the Au layer has to be a result of triplet formation.
- We therefore conclude that as with the muon result this induced moment is as a result of the triplet superconducting state.

Motivation

Bulk Spin Transfer Torque

- PRL **96,** 256601 (2006)
- PRB **79,** 104433 (2009)

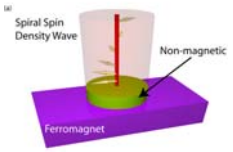

$$|f| = (1/2\pi J\hbar)\sqrt{(C_{23}j_3)^2 - (6K_6^6)^2}$$

Exotic Phase

- PRB **78,** 020402(R) (2008)
- PRB **79,** 134420 (2009)

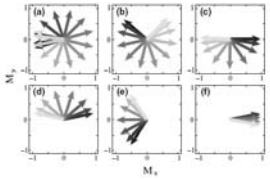

- Spin-triplet SC Science, **329,** 59 (2010)
- RMP **77** 1321 (2005)

Magnetic Spirals in Holmium thin films

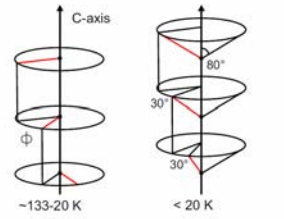

The representative magnetic structure of bulk Ho below its Néel temperature (left) and below its Curie temperature (right).

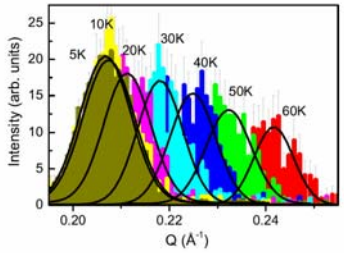

The momentum transfer versus the intensity of the magnetic diffraction peak for the 50 nm thick Ho sample as a function of temperature.

Bulk Ho Field Phase diagram

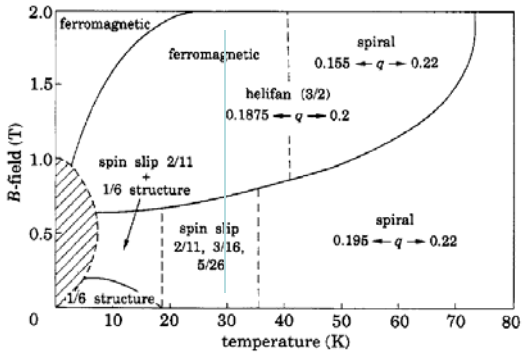

D. A Jehan *et al.*, Europhys. Letts. 17 553 (1992)

Polref: Diffuse scattering from a holmium spin spiral: 7.5T

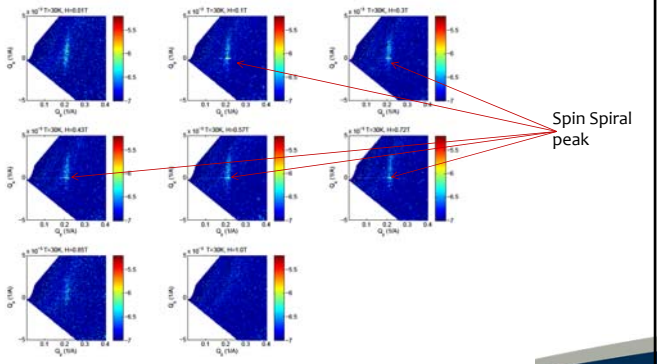

J. D. S. Witt et al. J Phys: Condens Matter **23,** 416006 (2011).

COHERENCE

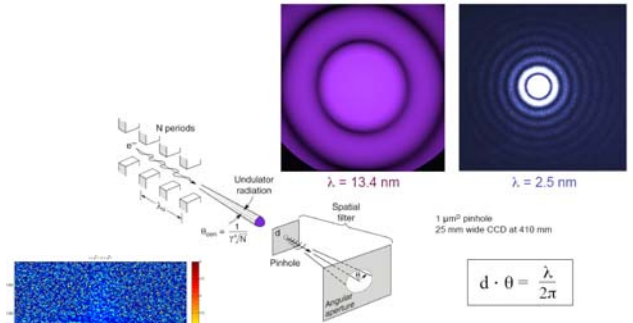

Hercules Sept 2015
Science & Technology Facilities Council ISIS

Lensless imaging of magnetic nanostructures by X-ray spectro-holography

S. Eisebitt[1], J. Lüning[2], W. F. Schlotter[1,2], M. Lörgen[1], O. Hellwig[1,3], W. Eberhardt[1] & J. Stöhr[2]

[1]BESSY mbH, Albert-Einstein-Straße 15, 12489 Berlin, Germany
[2]SSRL, Stanford Linear Accelerator Center, 2575 Sand Hill Road, Menlo Park, California 94025, USA
[3]Department of Applied Physics, 336 Via Pueblo Mall, Stanford University, Stanford, California 94305-4090, USA
[4]San Jose Research Center, Hitachi Global Storage Technologies, 650 Harry Road, San Jose, California 95120, USA

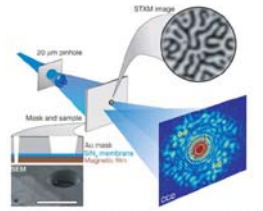

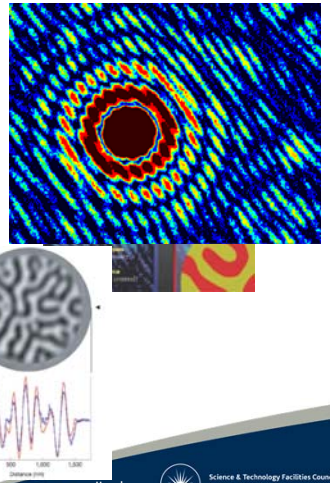

Figure 1 Scheme of the experimental set-up. Monochromatized and circular polarized X-rays are incident on a mask–sample structure after spatial coherence filtering. The object and reference beam are defined by the mask, and the resulting hologram is recorded on a CCD detector. The lower inset shows the geometry and an electron microscopy image of the mask–sample structure. The scale bar in the microscopy image is 2.0 μm. The top inset shows a STXM image of the magnetic structure illuminated through the sample aperture. The field of view is 1.5 μm.

Nature **432** 885 (2004)

Hercules Sept 2015
Science & Technology Facilities Council ISIS

Extended References

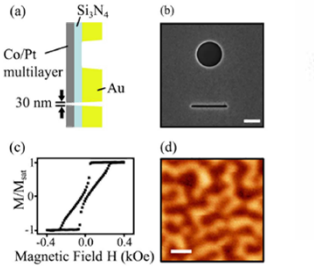

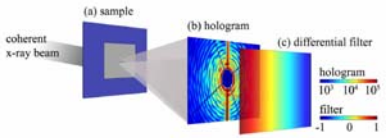

Fig. 2. (Color online) (a) The object and reference slit are illuminated by the coherent x-ray beam. (b) The hologram formed by the interference of the scattered x-rays from the object and reference slit is recorded on the CCD camera in the far field. (c) A linear differential filter, defined by the derivative of the slit direction, is multiplied by the hologram before performing a Fourier transform to retrieve the reconstructed image.

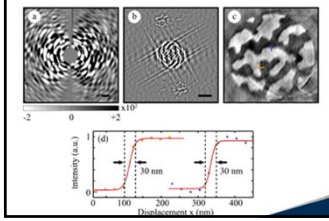

Duckworth, SL *et al.* Vol. 19, Optics Express 16223 (2011)
Duckworth, SL *et al. New J. Phys.* **15** 23045 (2013)

Hercules Sept 2015
Science & Technology Facilities Council ISIS

Speckle Cross-correlation Spectroscopy

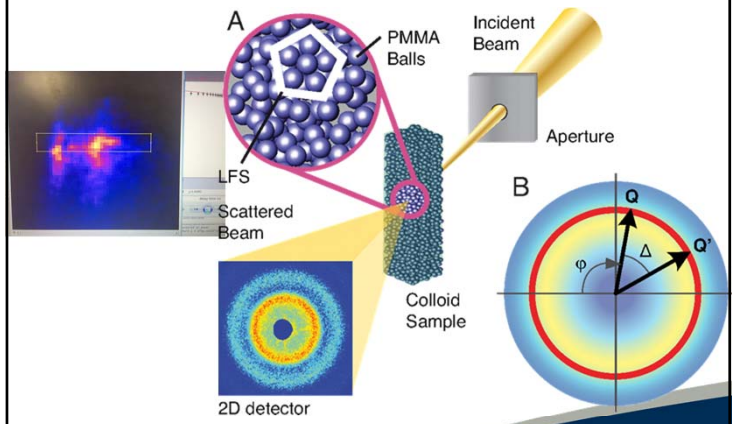

Proceedings of the National Academy of Sciences **106**, 11511-11514 (2009)

OxfordMaterials

NSLS

Stamping magnetic structures:

micro-contact printing

Stamping magnetic structures

- Micro-stamp production
- 200/200nm stripes
- 20nm high

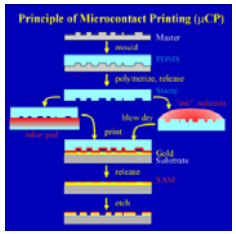

IBM Zurich

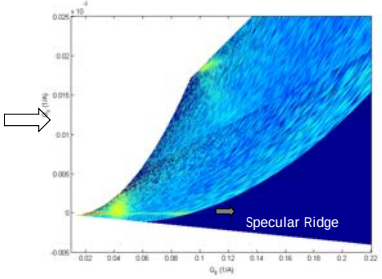

A. Kumar and G. M. Whitesides, Appl. Phys. Lett. **63**, 2002 (1993).

Co L_{III} resonance

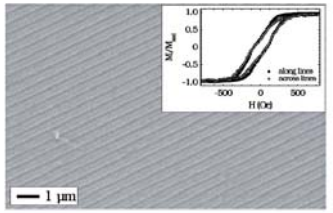

FIG. 1. A scanning electron micrograph of the sample. Inset is a Kerr loop of the sample with the field applied in the plane, both along (•) and across (○) the direction of the lines.

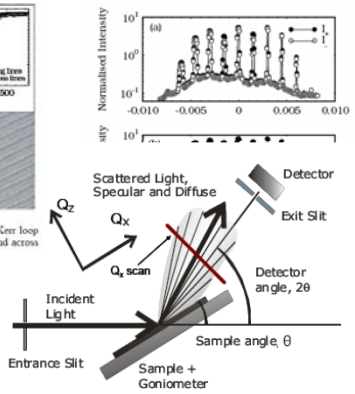

AFM/MFM Measurements

- MFM weak
  - Measured @remanence
- Xrms measures structure-charge correlation

$$\propto \mathrm{Re}(\widetilde{f_m} \cdot \widetilde{f_s})$$

- MFM sensitive to force gradients
- s-xrms magnetisation
- Magnetism tracks gross features

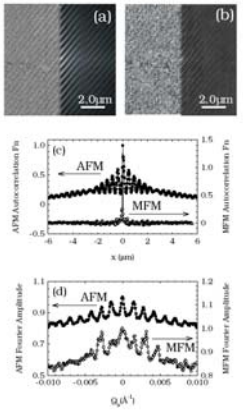

L-A Michez et al. APL **86** 112502 (2005)

Spin Asymmetry

$$f_n^{res} = \begin{pmatrix} 1 & 0 \\ 0 & \mathbf{k_i} \cdot \mathbf{k_f} \end{pmatrix} F_n^{(0)} + i \begin{pmatrix} 0 & -\mathbf{k_i} \cdot \mathbf{M_n} \\ \mathbf{k_f} \cdot \mathbf{M_n} & (\mathbf{k_i} \times \mathbf{k_f}) \cdot \mathbf{M_n} \end{pmatrix} F_n^{(1)}$$

$$I = Tr(f_n^{res} \cdot \rho \overline{f_n^{res\star}})$$

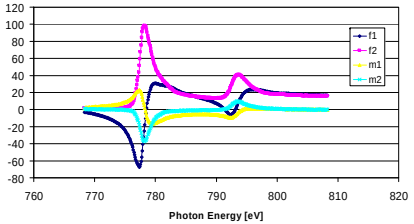

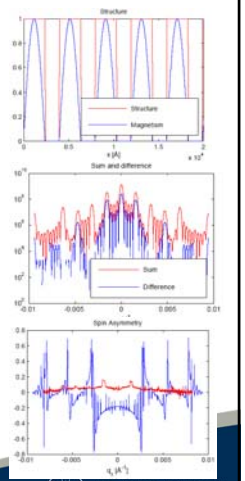

5 – 10μm Stripes

- H=H_C
- Domain size
  - χ=0° (||) 3.5μm
  - χ=90°(⊥) 4.4μm
- Domain Distribution
  - ~3rad
- No Magnetic Roughness

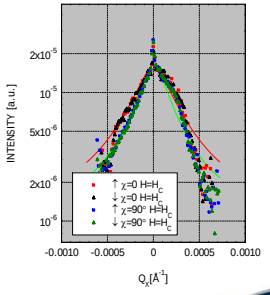

- H=H_{Sat}
- H || Stripes
- Integer order satellites
- Magnetic Roughness

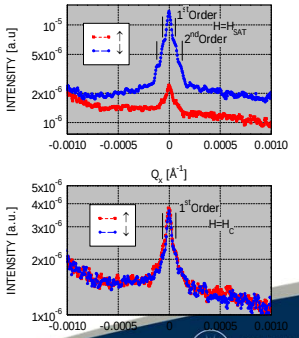

Structurally smooth- Magnetically Rough

out of plane anisotropy

NSLS

Out of plane Anisotropy

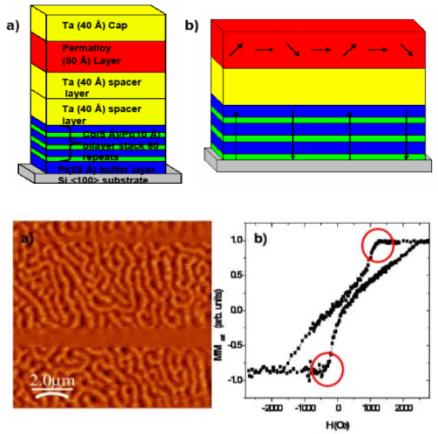

s-xrms

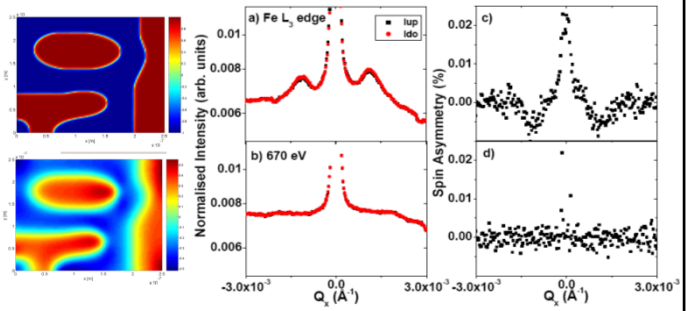

Accessing ip and oop

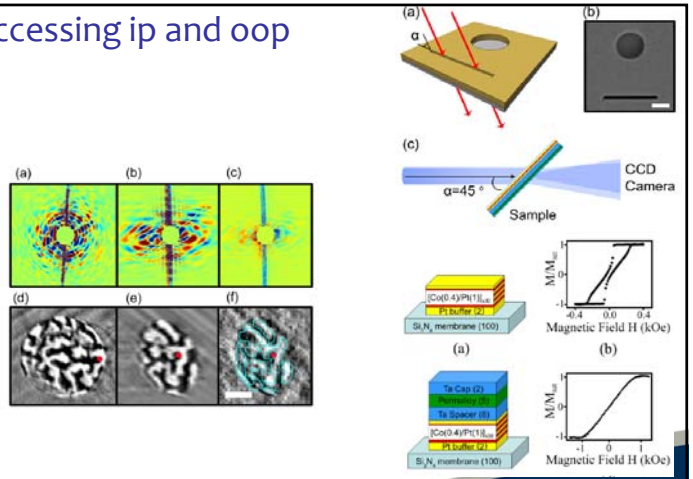

Conclusions

- **Diffuse Measurements**
  - Direct (simple) scattering cross-section allowing the quantitative analysis of the magnetic disorder
  - Statistical analysis of magnetic surface morphology not possible with other techniques
- **Dynospheres**
  - Increased coercivity
  - Patterning geometry does not affect AFM domain size
  - Magnetic roughness driven by the structural periodicity
    - *cf.* Smooth structural surfaces where the magnetic roughness is on a longer lengthscale than the structural in-plane correlation length
    - Free interfacial magnetisation
    - Fluctuation of surface moments
- **Stripes**
  - Domain size and disorder relatively independent of field direction
  - Magnetic roughness driven by the PMMA roughness
- **Proximity patterning**
  - Good qualitative agreement
  - Requires the neutron measurement
- **Ongoing/future Measurements**
  - Micromagnetic simulation of sphere/stripe structure
  - Dwba analysis

Artificial Spin Ice

- 2D array of single domain, ferromagnetic nanobars
- Ising axes defined by shape anisotropy
- Tailor lattice geometry to enforce frustration
- Square and kagome vertex systems analogous to crystalline “spin ice” materials
  - Frustrated bulk magnet
  - Coulombic magnetic “monopole” excitations
- Athermal (T_{active} ~ 10^5K), therefore, field-ordering currently main focus
- Magnetic microscopy – vertex statistics

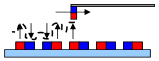

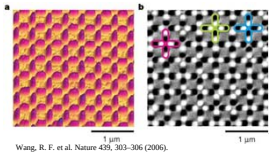

Wang, R. F. et al. Nature 439, 303–306 (2006).

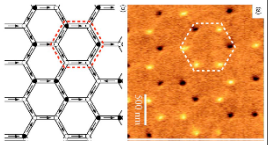

Tanaka et al. PRB 73, 052411 (2006).

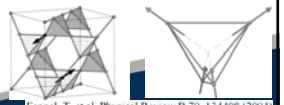

Fennel, T. et al. Physical Review B 70, 134408 (2004)

Magnetic Square Ice

- 2^4 = 16 possible vertex configurations
  - 4 vertex types
- 2-fold degenerate ground-state (GS)
- Studied statistically following applied fields

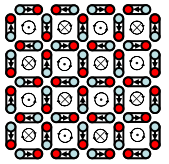

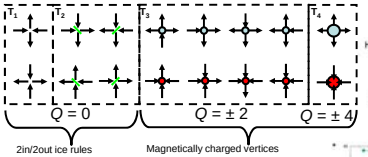

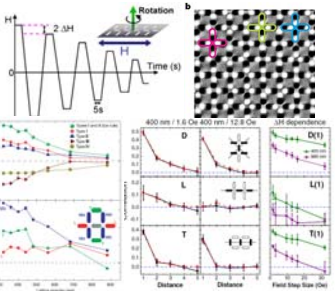

- ac demagnetization
- Energy minimisation
- Only short range correlated states accessed

Wang, R. F. et al. (2006) Nature 439, 303–306
Ke et al. (2008) PRL 101, 037205

ASi

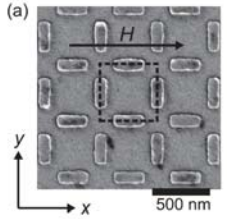

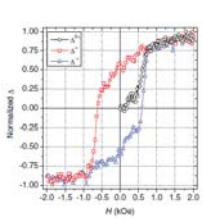

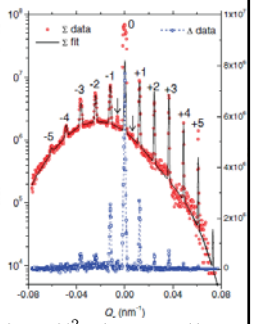

$$\sum(Q_x) = C \sum_{q_x, q_y} (|F(q_x, q_y)|^2 \, R(Q_x; q_x, q_y))$$

- Superposition of loops
- Advantages over Bragg-MOKE
- Opportunities to look at thermal systems

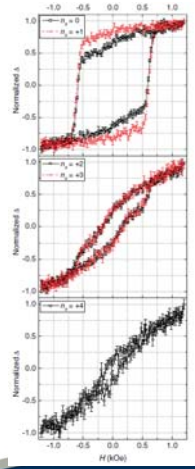

AIP Advances 2, 022163 (2012)

QUANTUM MATTER

QAHE & Topological Insulators (TIs)

- Quantum Hall effect observed in 2DEG
  - $\sigma = \nu \frac{e^2}{h}$
- Anomalous Quantum Hall effect (QAH)
  - Band inversion
  - Ferromagnetic insulator breaking TRS
- TIs possess insulating bulk gap and gapless edge states
  - Magnetic dopants

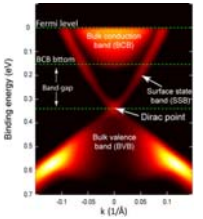

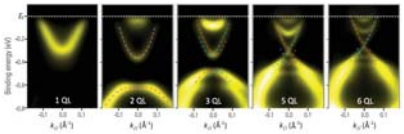

Yu et al. Science **329** (2010) 61
Chang et al. Science **3340** (2013) 167
He, K., Wang et al. *Natl. Sci. Rev.* **1**, 38–48 (2013)

Cr doped Bi_2Se_3

- Tc~20K for 5%
- Good crystalline quality ~<5%

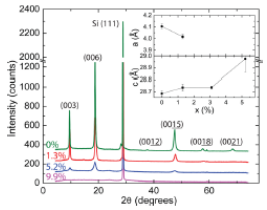

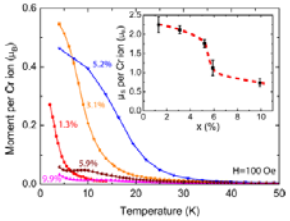

Haazen et al. APL **100** (2012) 082404

$(Cr_{0.12}Bi_{0.88})_2Se_3$

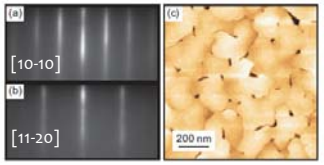

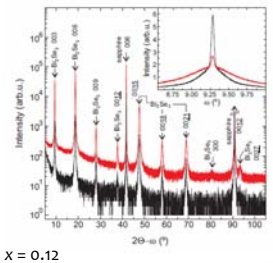

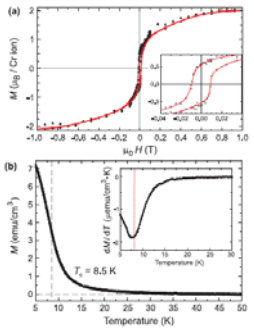

X = 0.12

- Cr concentration fixed by RBS
- 1.5μ_B/Cr @0.7T
- No enhancement observed in the near surface region
- Moment less than 3.78μ_B of Cr^{3+} substituted on Bi site

- **Summary**
- Cr doping up to 12% without a loss of crystallinity (substitutional doping)
- Moment lower (2.1) than expected for Cr^{3+}
- Homogeneous ferromagnetism
- Precursor to observing the QAHE (lower temperatures)

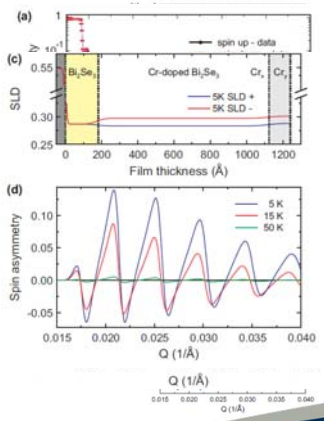

Collins-McIntyre, L. J. *et al.* Magnetic ordering in Cr-doped Bi_2Se_3 thin films. *Europhys. Lett.* **107**, 57009 (2014).

Summary

- Can take advantage of (*i.e.* control) the refractive index (polarised neutrons, deuteration, resonant enhancement and isotopic substitution)
- Can extract magnetic structures
- Realistic sample environments
  - Time resolution
  - Speckle
- Sub nm resolution for systems
- Lengthscales (out of plane) monolayer to ~100nm

Magnetism Summary

- Neutrons
  - see the B-field
  - Strong scattering
  - See component perpendicular to Q
  - Penetrating
  - Polarisation dependence
  - Simple cross-section
- Photons
  - Weak scattering (non-resonant)
  - Separation of orbital and spin
  - Large resonant enhancements
  - Polarisation dependence
  - Depth selectivity
  - Complex (rich) cross=section

Highly complementary probe for nanoscale magnetism

References

- Polarized Neutrons, W.G. Williams, Oxford (1988)
- Theory of Magnetic neutron and photon scattering, E. Balcar & S.W. Lovesey, Oxford (1988)
- Introduction to Thermal Neutron Scattering, G.L. Squires, Cambridge (1978)
- Elements of Modern X-Ray Physics, Als-Nielsen and McMorrow, Wiley & Sons (2001)
- Magnetism: from fundamentals to nanoscale dynamics, Stohr and Siegmann, Spinger (2006)

- www.ill.eu
- www.isis.stfc.ac.uk
- www.esrf.eu
- www.diamond.ac.uk

Review Articles


Report on Progress

X-rays and magnetism


Journal of Magnetism and Magnetic Materials

Neutron scattering—The key characterization tool for nanostructured magnetic materials

Fischer P and Ohldag H 2015 X-rays and magnetism: a review of program in magnetic studies with polarized soft x-rays *Reports Prog. Phys.* **78** 094501 (2015)
Fitzsimmons M R and Schuller I K 2014 Neutron scattering—The key characterization tool for nanostructured magnetic materials *J. Magn. Magn. Mater.* **350** 199–208 (2014)
Liu Y and Ke X 2015 Interfacial magnetism in complex oxide heterostructures probed by neutrons and x-rays J. Phys. Condens. Matter **27** 373003

Hercules
Sept 2015

Science & Technology Facilities Council
ISIS